Biological Control 208 (2025) 105853

Contents lists available at ScienceDirect

Biological Control

journal homepage: www.elsevier.com/locate/ybcon

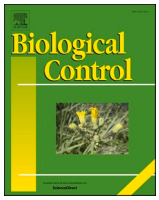

A novel *Arthrobotrys* species: Taxonomic characterization, nematicidal activity, and multi-omics insights into nematode predation

Mengting Gao [a,1], Zhaoqi Yan [a,1], Zexin Liu [a], Yunxia Jiang [a], Tengteng Liu [a], Xingjun Miao [b], Meixue Dai [a], Tanay Bose [c,*], Runlei Chang [a,d,*]

[a] College of Life Science, Shandong Normal University, Jinan, China
[b] Linyi Municipal Forestry Bureau,Linyi, China
[c] Department of Biochemistry, Genetics & Microbiology, Forestry and Agricultural Biotechnology Institute (FABI), University of Pretoria, Pretoria, South Africa
[d] Dongying Institute, Shandong Normal University, Dongying, China

HIGHLIGHTS

- Discovered novel nematode-trapping fungus Arthrobotrys byssisimilis.
- Achieved 100% pinewood nematode kill in 10–30 mins using culture filtrates and extracts.
- Shows strong tolerance to pine volatiles, ensuring better field adaptability.
- Genome shows 104 proteases, 8 chitinases as major virulence factors.
- Found 638 genes differentially expressed under nematode stress, stage-specific virulence.

ARTICLE INFO

Keywords:
Bursaphelenchus xylophilus
Biological control
CAZymes
Cytochrome P450
Secondary metabolites

ABSTRACT

Bursaphelenchus xylophilus, the pinewood nematode (PWN), is a devastating invasive pest responsible for widespread mortality in global conifer forests. During a survey of bark beetle-associated fungi, a nematode-trapping fungus was isolated from an empty beetle gallery in *Pinus thunbergii*. ITS sequence analysis suggested it represented a novel species. This study aimed to characterize the fungus taxonomically and evaluate its biocontrol potential against PWN. Multi-locus phylogenetic analyses (ITS, TEF1-α, RPB2) confirmed the isolate as a new species, *Arthrobotrys byssisimilis* sp. nov. Morphological examination revealed adhesive trapping networks and distinctive ellipsoidal conidia. Enzymatic assays demonstrated chitinase and protease activity, with optimal conditions defined for pH and temperature. Culture filtrates, protein extracts, and secondary metabolites showed rapid, dose-dependent nematicidal effects, achieving 100 % PWN mortality within 10–30 min. The fungus exhibited strong tolerance to pine-derived volatiles (α-pinene, β-pinene, turpentine, and ethanol), indicating high adaptability to the host environment. Whole-genome sequencing revealed a 36.97 Mb genome with 8,354 predicted genes, including 104 proteases, 8 chitinases, and diverse secondary metabolite biosynthesis clusters. Transcriptomic profiling after nematode exposure identified 638 differentially expressed genes, including virulence-related enzymes (proteases, CAZymes), cytochrome P450s, and PHI factors, with evidence of stage-specific regulation. *Arthrobotrys byssisimilis* is the first *Arthrobotrys* species reported from a bark beetle gallery, expanding the ecological scope of the genus. The integrated in vitro nematicidal activity, physiological adaptability, and multi-omics data suggest *A. byssisimilis* warrants further evaluation as a potential biocontrol agent against PWN, while its unique genomic features provide new molecular targets for investigating fungal-nematode interactions.

* Corresponding authors at: Department of Biochemistry, Genetics, and Microbiology, Forestry and Agricultural Biotechnology Institute (FABI), University of Pretoria, Pretoria, South Africa (T. Bose), and College of Life Science, Shandong Normal University, Jinan, China (R. Chang).
E-mail addresses: Tanay.Bose@fabi.up.ac.za (T. Bose), changrunlei@163.com (R. Chang).
[1] These authors have contributed equally to this work and share the first authorship.

https://doi.org/10.1016/j.biocontrol.2025.105853
Received 20 May 2025; Received in revised form 21 June 2025; Accepted 17 July 2025
Available online 21 July 2025

1. Introductions

Bursaphelenchus xylophilus, commonly known as the pinewood nematode (PWN), is a devastating phytopathogen responsible for pine wilt disease, causing severe ecological and economic losses to global forestry (Chen et al., 2024; Kim et al., 2020; Xiao et al., 2024). This invasive nematode disrupts water transport in conifers by feeding on parenchymal cells and forming symbiotic relationships with vector beetles, such as *Monochamus* spp., leading to rapid tree mortality (Back et al., 2024; Futai 2013). Efforts to control pinewood nematode disease focus on three main strategies: suppressing the *B. xylophilus* population, disrupting its insect vectors, and enhancing host tree resistance (Kim et al., 2020). Physical controls, such as heat treatment of infected wood and quarantine measures, aim to eliminate nematodes and prevent their spread (Kim et al., 2020). Chemical control relies on nematicides and insecticides to target PWN or its vectors, though concerns over environmental persistence and non-target toxicity limit their usage (Kim et al., 2020). Biological control offers a promising alternative utilizing natural antagonists like nematophagous organisms to suppress PWN populations (Kim et al., 2020). For example, species of *Arthrobotrys* have been shown to effectively control PWN populations (Wu et al., 2023; Yang et al., 2007b; Zhang et al., 2022b; Zhang et al., 2021).

Arthrobotrys is the largest and most diverse genus within the family Arthrobotryaceae (Orbiliales, Orbiliomycetes, Pezizomycotina, Ascomycota) of nematophagous fungi (Zhang et al., 2024a). Currently, the family comprises 78 accepted species as per the Species Fungorum (https://www.indexfungorum.org/). The genus *Arthrobotrys* was erected by Corda (1839) with *Arthrobotrys superbus* as the type species. This genus is characterised by bicellular conidia arranged in a whorl attached to the tip of sterigmata and on the nodes of the conidiophore (Corda, 1839). Much later, Drechsler (1933) refined the isolation technique for these nematophagous fungi, resulting in a surge of species discoveries. The genus was redefined based on characteristics such as branched or simple conidiophores and the asynchronous development of obovoid to pyriform conidia with 0–3 septa (Haard 1968; Schenck et al., 1977). Advancements in molecular biology have further elucidated the defining characteristics of *Arthrobotrys* species, particularly their ability to form adhesive networks that facilitate nematode capture (Li et al., 2005; Yang et al., 2012; Zhang et al., 2025a; Zhang and Hyde, 2014).

The morphological transition to adhesive networks in these fungi represents a critical phenotypic shift from saprophytic to predatory behaviour. The predation process comprises several distinct phases, such as chemotactic attraction, cuticular adhesion, mechanical penetration, and nematode immobilization (Lin et al., 2023; Wang et al., 2023). Upon contact with the host nematode, fungal hyphae undergo rapid morphological differentiation, reorienting perpendicular to the nematode surface. The subsequent cuticle penetration is then facilitated by a combination of mechanical force and enzymatic degradation, mediated by secreted hydrolases, ultimately leading to the formation of a penetration tube and successful host invasion (Wang et al., 2023).

Since nematodes and their eggshells are primarily composed of protein and chitin, research has focused on identifying extracellular enzymes, such as proteases and chitinases, that facilitate their degradation (Rahman et al., 2023; Vidal-Diez de Ulzurrun et al., 2024; Zhang et al., 2025b). For example, PII serine protease from *A. oligospora* has been characterized and cloned. Emerging data showed that its expression is induced by the presence of nematode cuticles (Ahman et al., 1996; Tunlid et al., 1994). Another serine protease, Aoz1, identified from the same fungus, shares a high similarity with PII (Zhao et al., 2004). Other nematophagous fungi, such as *A. microscaphoides* and *A. shizishanna,* also produce serine proteases homologous to those found in *A. oligospora* (Jia et al., 2024; Wang et al., 2006a; Wang et al., 2006b; Yang et al., 2007b). Serine proteases have been identified as key virulence factors, crucial for nematode infection (Yang et al., 2007a). This is exemplified by Ac1 identified from *A. conoides*, a homolog of PII and Aoz1, which has demonstrated nematode immobilization activity (Yang et al., 2007b). In addition to proteases, chitinases also play a significant role in nematode parasitism. Chitinases such as AO-379, AO-483, AO-492, and AO-801 have been shown to degrade nematode eggshells and cuticles, although they appear to lack immobilization capabilities (Gong et al., 2022; Gong et al., 2019; Zhang et al., 2024b; Zhong et al., 2019).

Fungi produce a variety of secondary metabolites, in addition to enzymes, that are also known to immobilize nematodes. Several nematicidal metabolites were identified from the culture filtrate of *A. thaumasia*, such as trimethyl-heptadien, dodecadienal, undecane, dibutyl-disulfide, paganin, talathermophilin, and dactylarin (Kassam et al., 2021). In *A. oligospora*, metabolites such as 1,2-benzenedicarboxylic acid, bis (2-methylpropyl) ester, (M) 1,4-benzenedicarboxylic acid, bis (2-methylpropyl) ester, and (M) decanedioic acid (2-ethylexyl) ester have been suggested as potential contributors to nematicidal activity (Bahena-Nuñez et al., 2024). Similarly, coumarins isolated from the culture filtrate of *A. musiformis* have been implicated in killing *Haemonchus contortus* infective larvae (Pérez-Anzúrez et al., 2022). Additionally, sesquiterpenyl epoxy-cyclohexenoids from *A. oligospora* are known to have both nematicidal and antibacterial activity (Teng et al., 2020). The biosynthesis of many of these secondary metabolites is regulated by genes encoding polyketide synthase (PKS) and polyketide-terpenoid (PK-TP) pathways, which play a pivotal role in the production of many secondary metabolites (Chen et al., 2020; Teng et al., 2020; Xu et al., 2016).

The multifaceted nematode-predation strategies of *Arthrobotrys* likely explain its broad scientific interest. At the moment, four commercially available biological nematicides, Royal 300 (Cayrol et al., 1978), Royal 350 (Cayrol 1983), Adx-1004 (Noweer 2014), and REM G® (Tranier et al., 2014), have been successfully developed using nematophagous fungi *A. robusta*, *A. irregularis*, *A. dactyloides*, and *Arthrobotrys* spp., respectively. Despite these successful applications, the molecular mechanisms underlying their nematicidal activity remain partially understood. This underscores the need for further research within the framework of biological control.

The advent of omics technologies has transformed our understanding of the molecular mechanisms governing fungal parasitism and pathogenicity. *Arthrobotrys oligospora* was the first fungal species in the Arthrobotryaceae to undergo whole-genome sequencing (Yang et al., 2011). Now, genomic data is available for nine *Arthrobotrys* species (Zhang et al., 2024c). Genomic analyses of *A. oligospora* have identified several virulence-related genetic elements, such as (i) putative Pathogen-Host Interaction (PHI) genes, (ii) subtilisin-like serine proteases, and (iii) key secondary metabolite biosynthesis enzymes (PKSs, NRPSs, and cytochrome P450s) (Yang et al., 2011). Subsequent functional studies have validated the roles of specific gene clusters in nematode predation, such as the PKS-PTS gene cluster (Chen et al., 2022; He et al., 2021; Zhou et al., 2022) and P450 genes (Song et al., 2017; Teng et al., 2020). These genomic studies provide the fundamental blueprint for understanding the evolutionary adaptations and biocontrol potential of nematophagous fungi.

Complementing genomic insights, transcriptomic studies have significantly advanced our understanding of the biology of *Arthrobotrys*. Before the sequencing of *A. conoides*, transcriptome analyses revealed 556 proteins matching the PHI database and 91 homologs of known virulence factors (Ramesh et al., 2015). More recent studies have further elucidated the transcriptional responses of *Arthrobotrys* species to various environmental stimuli, such as temperature fluctuations (Jia et al., 2024), glucose availability (Liu et al., 2020), chitin exposure (Li et al., 2024), ammonia stress, and nematode interactions (Liang et al., 2013; Yang et al., 2022). These transcriptomic profiles are crucial for identifying condition-specific virulence factors, which can inform the development of more targeted and effective biocontrol strategies.

During a survey of bark beetle-associated fungi from coniferous trees in Shandong province of China, isolate CGMCC 3.20358 was recovered and putatively identified as an undescribed *Arthrobotrys* species using the ITS gene region through a sequence similarity search against the

NCBI database. This study was conceptualized to classify this putative new species and evaluate its biocontrol potential against PWN. To achieve this, we conducted multi-locus phylogenetics, enzymatic profiling, and bioassays. To further explore the molecular basis of its nematode predation, we performed whole-genome sequencing coupled with transcriptomic analysis. We hypothesized that the new *Arthrobotrys* species kills nematodes using enzymes and secondary metabolites, which are partly triggered by the presence of nematodes, and that it can survive in pine tree environments. As the first *Arthrobotrys* isolated from bark beetle galleries, *A. byssisimilis* exhibits unprecedented pine ecosystem compatibility coupled with rapid PWN lethality, positioning it as a uniquely adapted biocontrol candidate.

2. Material and methods

2.1. Fungal isolation

A single isolate of the nematophagous fungus was recovered from an empty beetle gallery on *Pinus thunbergii* collected from Fei County, near Linyi city (35°20′ N, 117°52′ E; altitude: 119.5 m asl), Shandong province of China. Mycelia from the beetle gallery were transferred onto Petri plates containing 2 % malt extract agar (MEA) amended with 0.05 % streptomycin. Single-hyphal tip isolation was used to generate a pure culture of the fungus. The ex-holotype culture of the nematophagous fungus was submitted to the China General Microbiological Culture Collection Center (CGMCC), and the holotype to the Herbarium Mycologicum, Academiae Sinicae (HMAS), Beijing, China.

2.2. DNA extraction, PCR amplification and sequencing

The total genomic DNA was extracted from five-day-old cultures growing on MEA using the PrepMan™ Ultra Sample Preparation Reagent (Applied Biosystems, Foster City, CA) following the manufacturer's protocol. The complete internal transcribed spacer (ITS) region, partial elongation factor 1-α (TEF1-α) genes, and the RNA polymerase II subunit B (RPB2) were amplified using the primer pairs ITS1F/ITS4 (Gardes and Bruns 1993; White et al., 1990), EF2F/EF2R (Jacobs et al., 2004; Marincowitz et al., 2015), and RPB2-6F/RPB2-7R (Liu et al., 1999), respectively.

Each 25 μL PCR reaction included 12.5 μL of 2 × Taq Master Mix (buffer, dNTPs, and Taq polymerase; Vazyme Biotech Co., Ltd, China), 0.5 μL each of forward and reverse primer, 10.5 μL of PCR-grade water, and 1 μL of DNA template. The PCR amplifications of all three gene regions were conducted with an initial denaturation at 95 °C for 3 min, followed by 30 cycles of 95 °C for 60 s, 55 °C for 60 s, 72 °C for 1 min, and a final elongation at 72 °C for 10 min. Positive amplifications were verified using 1.5 % agarose gel electrophoresis.

Bidirectional sequencing of all PCR products using the above-mentioned primers was outsourced to Sangon Biotech Co., Ltd. The forward and the reverse sequences for each gene region were assembled using Geneious v7.1.4 (Biomatters, Auckland, New Zealand). Preliminary identification of the fungus was done using BLAST (Altschul et al., 1990) available through the NCBI GenBank.

2.3. Phylogenetic analyses

The isolate was preliminarily identified as an undescribed species of *Arthrobotrys* using the ITS gene region. Thus, for the phylogenetic identification of the nematophagous fungus, separate datasets were compiled for three gene regions: ITS (72 taxa), TEF1-α (48 taxa), and RPB2 (50 taxa). These datasets included sequences generated in this study, along with those from ex-type isolates of previously described *Arthrobotrys* species retrieved from the NCBI GenBank (Table 1). The sequences were aligned using MAFFT v7.526 (Katoh and Standley 2013), and manually refined using MEGA v12 (Tamura et al., 2013). A concatenated dataset was generated using FASconCAT (Kück and Meusemann 2010).

Model testing, maximum likelihood (ML), and Bayesian inference (BI) analyses were done through the CIPRES Science Gateway version 3.3 (Miller et al., 2010). jModelTest version 2.1.6 (Darriba et al., 2012) was used to select the most suitable substitution models for both single genes and concatenated datasets. ML analyses were conducted using RaxML version 8.2.4 (Stamatakis 2014) with the GTR + Gamma substitution model and 1000 bootstrap replicates. BI analyses were performed using MrBayes version 3.2.6 (Ronquist et al., 2012), with four MCMC chains initiated from a random starting tree and run for five million generations, sampling trees every 100th generation. A quarter of the sampled trees were discarded as burn-in, and the remaining trees were used to construct the majority rule consensus trees. Maximum Parsimony (MP) analyses were conducted using MEGA-X (Kumar et al., 2018), treating gaps as a fifth character in the analysis. All the sequence alignments and resulting phylogenetic trees are deposited at Mendeley Data (https://doi.org/10.17632/mfty8jdvpw.1).

2.4. Growth and morphological studies

The ex-type isolate of the nematophagous fungi was sub-cultured on MEA and incubated for seven days at 25 °C in the dark. Thereafter, 5 mm agar plugs were placed at the centers of 90 mm Petri dishes, and three replicate plates per isolate were incubated at 5, 10, 15, 20, 25, 30, and 35 °C (± 0.5 °C) in the dark. The colony diameter was measured at an interval of two days up to the tenth day.

To induce trapping structures, the pure culture was transferred to fresh 2 × 2 cm observation wells on cornmeal agar (CMA) plates, which were created by scooping out agar with a sterile needle. The plates were incubated at 26 °C until the mycelium colonized the wells. Then, ~1000 live PWN were introduced to stimulate trapping structure development.

Microscopic structures were measured and photographed using a Zeiss Axio Imager Z2 (Carl Zeiss, Germany). Fifty measurements for each taxonomically informative structure were made, such as conidiophore and conidia. The measurements are presented in the format (minimum–) mean minus standard deviation–mean plus standard deviation (–maximum). The trapping structures were photographed using a Zeiss Axio Imager Z2 (Carl Zeiss, Germany) and a TM3030 scanning electron microscope (Hitachi, Japan).

2.5. Preparation of liquid culture filtrate

The isolate of the nematophagous fungus was inoculated on the MEA and incubated at 28 °C for 7 days. Three agar plugs with mycelia were inoculated into 100 mL LMZ liquid medium (2 g gelatin, 8 g peptone, 1 g yeast extract, 0.5 g $(NH_4)_2SO_4$, 0.01 g $FeSO_4{\cdot}7H_2O$, 0.5 g $MgSO_4{\cdot}7H_2O$ in 1 L phosphate buffer [pH 6.5, $Na_2HPO_4{\cdot}12H_2O$ / $NaH_2PO_4{\cdot}2H_2O$]) (Schenck et al., 1980) and incubated at 28 °C, 180 rpm for six days in darkness. The liquid culture filtrate was first filtered through cheesecloth to remove mycelial debris, then centrifuged at 10,000 rpm for 15 min to obtain the supernatant. Finally, it was filtered through a 0.22 μm membrane to remove spores and other cellular debris, and the filtrate was collected and stored at −20 °C inside a refrigerator.

2.6. Chitinase and protease activity assay

Chitinase activity was measured using the dinitrosalicylic acid (DNS) method (Miller 1959), with colloidal chitin as the substrate. A 600 μL filtrate was mixed with an equal volume of 1 % colloidal chitin and incubated at 35 °C for 30 min. The reaction was stopped by boiling the mixture for 15 min. After centrifugation at 12,000 rpm, 1 mL of this supernatant was mixed with 2 mL of DNS reagent and boiled for 5 min to develop color. The mixture was then diluted with 9 mL of distilled water, and absorbance was measured at 540 nm using a UV–visible spectrophotometer (X-5, Metash, China). Each treatment was performed in triplicate and repeated once for consistency. For the control, the filtrate

Table 1
A list of *Arthrobotrys* species with respective GenBank accession numbers for ITS, TEF1-α, and RPB2 gene regions used in the phylogenetic studies. *Dactylellina cangshanensis* and *D. yushanensis* served as the outgroup taxa.

Taxon	Strain Number	GenBank accession Number		
		ITS	TEF1-α	RPB2
Arthrobotrys amerospora	CBS 268.83^{T}	NR_159625	—	—
Arthrobotrys angiopteridis	KUNCC 23–14121 ^{T}	PQ346307	—	PQ356383
Arthrobotrys angiopteridis	KUNCC 23–14119	PQ346306	—	—
Arthrobotrys anomala	YNWS02-5–1	AY773451	AY773393	AY773422
Arthrobotrys arthrobotryoides	AOAC	MF926580	—	—
Arthrobotrys blastospora	CGMCC 3.20940^{T}	OQ332405	OQ341651	OQ341649
Arthrobotrys botryospora	CBS 321.83^{T}	NR_159626	—	—
Arthrobotrys byssisimilis	**CGMCC3.20358^{T}**	**PP476591**	**PP481404**	**PV295287**
Arthrobotrys cibiensis	DLUCC 109	OR880379	OR882792	OR882797
Arthrobotrys cladodes	1.03514	MH179793	MH179616	MH179893
Arthrobotrys clavispora	CBS 545.63^{T}	MH858353	—	—
Arthrobotrys conoides	670	AY773455	AY773397	AY773426
Arthrobotrys cookedickinson	YMF 1.00024	MF948393	MF948550	MF948474
Arthrobotrys cystosporia	CBS 439.54	MH857384	—	—
Arthrobotrys dendroides	YMF 1.00010	MF948388	MF948545	MF948469
Arthrobotrys dianchiensis	1.00571	MH179720	—	MH179826
Arthrobotrys elegans	1.00027	MH179688	—	MH179797
Arthrobotrys eryuanensis	CGMCC 3.19715^{T}	MT612105	OM850307	OM850301
Arthrobotrys eudermata	SDT24	AY773465	AY773407	AY773436
Arthrobotrys flagrans	1.01471	MH179741	MH179583	MH179845
Arthrobotrys gampsospora	CBS 127.83	U51960	—	—
Arthrobotrys globospora	1.00537	MH179706	MH179562	MH179814
Arthrobotrys gongshanensis	CGMCC 3.23753^{T}	OM801277	OM809162	OM809163
Arthrobotrys guizhouensis	YMF 1.00014	MF948390	MF948547	MF948471
Arthrobotrys heihuiensis	DLUCC 108–1	OR880378	OR882791	OR882796
Arthrobotrys hengjiangensis	CGMCC 3.24983^{T}	OQ946587	OQ989312	OQ989302
Arthrobotrys hyrcanus	IRAN 3650C	MH367058	OP351540	—
Arthrobotrys indica	YMF 1.01845	KT932086	—	—
Arthrobotrys iridis	521	AY773452	AY773394	AY773423
Arthrobotrys janus	85–1	AY773459	AY773401	AY773430
Arthrobotrys javanica	105	EU977514	—	—
Arthrobotrys jindingensis	CGMCC 3.20895^{T}	OP236810	OP272511	OP272515
Arthrobotrys jinpingensis	CGMCC 3.20896^{T}	OM855569	OM850311	OM850305
Arthrobotrys jinshaensis	DLUCC 133	OR880381	OR882794	OR882799
Arthrobotrys koreensis	C45	JF304780	—	—
Arthrobotrys lanpingensis	CGMCC 3.20998^{T}	OM855566	OM850308	OM850302
Arthrobotrys latispora	H.B. 8952	MK493125	—	—
Arthrobotrys longiphora	1.00538	MH179707	—	MH179815
Arthrobotrys luquanensis	CGMCC 3.20894^{T}	OM855567	OM850309	OM850303
Arthrobotrys luzhangensis	CGMCC 3.20941^{T}	OK643973	OM621809	OM621810
Arthrobotrys mangrovispora	MGDW17	EU573354	—	—
Arthrobotrys megalospora	TWF800	MN013995	—	—
Arthrobotrys microscaphoides	YMF 1.00028	MF948395	MF948552	MF948476
Arthrobotrs multiformis	CBS 773.84^{T}	MH861834	—	—
Arthrobotrys musiformis	SQ77-1	AY773469	AY773411	AY773440
Arthrobotrys musiformis	1.03481	MH179783	MH179607	MH179883
Arthrobotrys nonseptatus	YMF 1.01852^{T}	FJ185261	—	—
Arthrobotrys obovata	YMF 1.00011^{T}	MF948389	MF948546	MF948470
Arthrobotrys oligospora	920	AY773462	AY773404	AY773433
Arthrobotrys paucispora	ATCC 96,704	EF445991	—	—
Arthrobotrys polycephala	1.01888	MH179760	MH179592	MH179862
Arthrobotrys pseudoclavata	1130	AY773446	AY773388	AY773417
Arthrobotrys psychrophila	1.01412	MH179727	MH179578	MH179832
Arthrobotrys pyriformis	YNWS02-3–1	AY773450	AY773392	AY773421
Arthrobotrys reticulata	CBS 550.63	MH858355	—	—
Arthrobotrys robusta	nefuA4	MZ326655	—	—
Arthrobotrys salina	SF 0459	KP036623	—	—
Arthrobotrys scaphoides	1.01442	MH179732	MH179580	MH179836
Arthrobotrys shizishanna	YMF 1.00022	MF948392	MF948549	MF948473
Arthrobotrys shuifuensis	CGMCC 3.19716^{T}	MT612334	OM850306	OM850300
Arthrobotrys sinensis	105–1	AY773445	AY773387	AY773416
Arthrobotrys sphaeroides	1.0141	MH179726	MH179577	MH179831
Arthrobotrys superba	127	EU977558	—	—
Arthrobotrys thaumasia	917	AY773461	AY773403	AY773432
Arthrobotrys tongdianensis	CGMCC 3.20942^{T}	OP236809	OP272509	OP272513
Arthrobotrys vermicola	629	AY773454	AY773396	AY773425
Arthrobotrys weixiensis	CGMCC 3.24984^{T}	OQ946585	OQ989310	OQ989300
Arthrobotrys xiangyunensis	YXY10-1^{T}	MK537299	—	—
Arthrobotrys yangbiensis	DLUCC 36–1	OR880382	OR882795	OR882800
Arthrobotrys yangjiangensis	DLUCC 124	OR880380	OR882793	OR882798
Arthrobotrys yunnanensis	A22^{T}	AY50993	—	—
Arthrobotrys zhaoyangensis	CGMCC 3.20944^{T}	OM855568	OM850310	OM850304
Dactylellina cangshanensis	CGMCC 3.19714^{T}	MK372062	MN915115	MN915114
Dactylellina yushanensis	CGMCC 3.19713^{T}	MK372061	MN915113	MN915112

was first inactivated by boiling before adding the substrate and then processed as above.

Protease activity was determined using the Folin-phenol reagent method (Wang and Pang 1981). Casein (1 % w/v) and trichloroacetic acid (TCA, 0.4 M) solutions were preheated at 40 °C for 5 min. One mL filtrate was incubated at 40 °C for 2 min before adding 1 mL of casein. After 10 min, the reaction was stopped by adding 2 mL of TCA. The mixture was left at room temperature for 3 min, then centrifuged at 12,000 rpm for 3 min. To the 1 mL supernatant, 5 mL Na_2CO_3 (0.4 M) and 1 mL Folin-phenol reagent were added, mixed thoroughly, and incubated at 40 °C for 20 min. After cooling, absorbance was measured at 680 nm using a spectrophotometer. Each treatment was performed in triplicate and repeated once for consistency. For the control, the filtrate was inactivated with TCA before adding the substrate and then processed as above.

Enzyme activities were assessed at 15, 25, 35, 45, and 55 °C (pH 7.0). The effect of pH was tested at 2, 4, 6, 8, and 10, using the optimal temperature determined earlier. The highest activity was set as 100 %, with relative activities calculated accordingly.

2.7. Nematicidal activity assay of liquid culture filtrate

The concentration gradient was systematically optimized based on preliminary range-finding tests adapted from Naz et al., (2021) and Özdemir and Arici (2021), where initial evaluations using 25 %, 50 %, 75 % and 100 % concentrations demonstrated ≥ 80 % mortality at ≥ 25 % concentration within 30 min of exposure. Based on these results, we refined the concentration series by eliminating the 75 % concentration while incorporating 12.5 % and 6.25 % dilutions to better characterize the dose–response relationship at sublethal levels, ultimately establishing a five-point concentration gradient (100 % [undiluted], 50 %, 25 %, 12.5 %, and 6.25 %) in sterile deionized water that enables comprehensive assessment of nematicidal activity across the full efficacy spectrum. One mL of each dilution was added to a 24-well cell culture plate, along with 100 second-stage (5 μL) PWN juveniles per well. A blank control included a sterile liquid culture medium. Each concentration had five replicates. Nematode viability was assessed using posture observation and the needle prick test. Mortality was recorded at 1-, 3-, 5-, 15-, and 30-min post-treatment. The percentage mortality rate (%) was calculated as (Number of dead nematodes / Number of nematodes added) × 100 %.

2.8. Nematicidal activity assay of protein concentrate

The fungal liquid culture filtrate was centrifuged at 4 °C, 4000 rpm for 20 min. The supernatant was stirred in an ice bath while saturated ammonium sulfate was added (4.6:1 ratio) to reach a concentration of 3.2 M. After overnight precipitation at 4 °C, the mixture was centrifuged at 2000 rpm for 20 min to collect the protein precipitate.

The precipitate was dissolved in 25 mM Tris-HCl and dialyzed at 4 °C for 24 h, with buffer changes every 3 h. The protein concentrate was diluted to 100, 50, 25, 12.5, and 6.25 % concentrations, following the protocol used for diluting liquid culture filtrate.

2.9. Nematicidal activity assay of secondary metabolites

The fungal liquid culture filtrate was concentrated to one-third of its volume by rotary evaporation at 60–65 °C, 70 rpm. It was then mixed with three times its volume of anhydrous ethanol and left at 4 °C overnight. The mixture was centrifuged at 5000 rpm, 4 °C for 20 min to remove proteins, starch, and large molecules. The supernatant was further concentrated under reduced pressure until no volume reduction occurred.

The concentrate was diluted to 100, 50, 25, 12.5, and 6.25 % concentrations and tested using the protocol for diluting liquid culture filtrate.

2.10. Assessment of fungal growth in the presence of antimicrobials

To evaluate the impact of plant volatile compounds on the growth of nematophagous fungus, inoculum plugs (3 mm) were placed at the center of 90 mm MEA plates containing ethanol at 0.5 %, 1 %, 2.5 %, and 5 %, with MEA alone as a control.

For volatile exposure, α-pinene (98 %), β-pinene (98 %), and turpentine were applied in varying volumes (0.5, 5, 50, and 500 μL) onto sterile gauze, which was attached to the Petri dish lids. Plates were sealed with Parafilm, placed in self-sealing bags, and incubated at 25 °C. Sterile distilled water served as the control. Each treatment was replicated three times.

Fungal growth was monitored daily, and colony diameter was marked on the reverse of the Petri plate. At the end of the experiment, mycelial migration and colony conditions were recorded to assess the effect of volatiles on the nematophagous fungus.

2.11. Statistical analyses

Data from the above assays were analyzed using one-way ANOVA. When variances were homogeneous, LSD and Tukey's HSD tests were used for post-hoc comparisons; otherwise, Dunnett's T3 and Tamhane's T2 tests were applied. Analyses were performed in IBM SPSS Statistics 20, and graphs were generated using Origin 2020.

2.12. Whole genome sequencing, assembly and annotation

The genome of the nematophagous fungus was sequenced using the Illumina NovaSeq platform by Shanghai Personalbio Technology Co., Ltd. Raw reads were quality-checked with FastQC v0.12.0 (https://www.bioinformatics.babraham.ac.uk/ projects/fastqc/) and processed with AdapterRemoval v2 (Schubert et al., 2016) to remove adapters. SOAPec v2.0 (Luo et al., 2012) performed quality trimming using a k-mer setting of 17. *De novo* assembly was done using A5-MiSeq v20160825 (Coil et al., 2014) and SPAdes v2.03 (Bankevich et al., 2012), followed by error correction with Pilon v1.18 (Walker et al., 2014). Genome completeness was assessed using BUSCO v3.0.2 (Waterhouse et al., 2018).

Repeat sequences were annotated using RepeatMasker v4.0.5 (Tempel 2012) with the Repbase database v20150807 (Kapitonov and Jurka 2008). *De novo* annotation was performed with RepeatModeler v1.0.4 (Smit and Hubley), incorporating RECON v1.0.8 (Bao and Eddy 2002) and RepeatScout v1.0.5 (Price et al., 2005). tRNA genes were predicted with tRNAscan-SE v1.3.1 (Lowe and Eddy 1997), rRNA genes with RNAmmer v1.2 (Lagesen et al., 2007), and other non-coding RNAs via Rfam comparisons (Griffiths-Jones et al., 2005).

Gene models were predicted using Augustus v3.03 (Stanke and Morgenstern 2005), GlimmerHMM v3.0.1 (Majoros et al., 2004), and GeneMark-ES v4.35 (Ter-Hovhannisyan et al., 2008), with homologous predictions from Exonerate v2.2.0 (Slater and Birney 2005). EvidenceModeler vr2012-06–25 (Haas et al., 2008) integrated all predictions. CAZy enzyme genes were identified using HMMscan v3.1b2 (Krogh et al., 1994). Antibiotic resistance genes were detected via BLAST against the CARD database (McArthur et al., 2013), and virulence factors against the DFVF database (Lu et al., 2012). Signal peptides were predicted with SignalP v5.0 (Almagro Armenteros et al., 2019), and transmembrane domains with TMHMM v2.0, allowing the identification of secreted proteins.

Protein-coding genes were annotated using DIAMOND v0.9.10.111 (Buchfink et al., 2015) against the NCBI nr database (release 2017.10.10). Further annotations included eggNOG-mapper (Huerta-Cepas et al., 2017) for functional classification, KEGG KAAS v2.1 (Moriya et al., 2007) for pathway mapping, Swiss-Prot for curated protein data, and InterProScan v66.0 (Finn et al., 2016) for Gene Ontology (GO) terms. BLASTP v2.5.0 + identified P450 genes, transporters, domains, and pathogen-host interaction factors.

Specific enzymes (e.g., lectins, proteinases, chitinases, cellulases, cellobiohydrolases, and pectinesterases) were manually curated. Serine protease families were screened based on structural similarities. Secondary metabolite biosynthetic genes, including PKSs and NRPSs, were identified using antiSMASH v7.0 (Blin et al., 2023).

2.13. Transcriptome sequencing and analyses

At 36 h post-induction with *B. xylophilus*, the nematophagous fungus formed three-dimensional adhesive nets, marking the selected time point for transcriptome analysis. One hundred second-stage *B. xylophilus* juveniles were added to a 4-day-old fungal culture and incubated at 28 °C for 36 h. The control group received sterile water. Mycelia were collected and flash-frozen in liquid nitrogen for 15 min and transported on dry ice to Wuhan OneMore Technology Co., Ltd. for sequencing.

Paired-end clean reads were aligned to the reference genome using STAR v2.7.5a (Dobin et al., 2013). Gene expression was quantified with HTSeq v0.12.4 (Anders et al., 2015). Principal Component Analysis (PCA) assessed sample clustering and group differences. Differential expression analysis was conducted using DESeq2 v3.11 (Wang et al., 2010). Gene Ontology (GO) and KEGG pathway enrichment of differentially expressed genes were analyzed with the 'clusterProfiler' package available through R v3.6.0 (Yu et al., 2012).

3. Results

3.1. Phylogenetic analyses

The concatenated dataset comprised 2,210 base pairs (ITS: 1–775, EF: 776–1371, RPB2: 1372–2210) from 72 sequences, including all *Arthrobotrys* species with valid sequence data, as well as the outgroup species *Dactylellina cangshanensis* and *D. yushanensis*. In this phylogenetic reconstruction, isolate CGMCC 3.20358 formed a sister relationship to a clade comprising *A. anomala* and *A. dendroides* (Fig. 1). This relationship received moderate support in the ML analysis (89 % bootstrap) but no significant support from the BI analysis. While similar topologies were recovered in the ITS and TEF1-α gene trees with strong branch support (Figs. S1, S2), the RPB2 gene tree (Fig. S3) showed a different placement, grouping CGMCC 3.20358 with *A. dendroides* and *A. polycephala* instead.

The reduced branch support in the concatenated tree, especially the lack of concordant support from BI analysis, likely reflects conflicting phylogenetic signals among the individual loci. Specifically, the incongruence between the RPB2 tree and the ITS/TEF1-α topologies suggests possible gene tree discordance, which may arise from processes such as incomplete lineage sorting, introgression, or differential evolutionary rates across loci. Additionally, RPB2 is a more conserved marker relative to ITS and TEF1-α, and may not resolve recent divergences with high precision, thereby introducing uncertainty in combined analyses. This discordance diminishes overall confidence in the precise placement of CGMCC 3.20358 and indicates that while it is closely related to members of the *A. anomala–A. dendroides* clade, its exact phylogenetic position remains unresolved without additional genomic or multilocus data.

3.2. Taxonomy

Arthrobotrys byssisimilis* R.L. Chang &Y.X. Jiang, *sp. nov. Fig. 2
MycoBank: MB852540.

Etymology. The fungal colony on MEA appears cotton-like, as reflected in its Latin name, *byssisimilis*, meaning "resembling cotton."

Holotype. CHINA. Shandong province: Fei county, Linyi city (35°20′ N, 117°52′ E), from the gallery of unknown beetle species on *Pinus thunbergii*, 5 May 2020, T. T. Liu & X. J. Miao; holotype = HMAS 352341, ex-holotype (living culture) CGMCC 3.20358 = SNM 231. Sequence data ITS = PP476591, TEF1-α = PP481404, and RPB2 = PV295287.

Diagnosis. *Arthrobotrys byssisimilis* differs from its sister species, *A. dendroides* and *A. anomala*, in terms of conidial morphology.

Culture characteristics. The colony exhibits a white, cotton-like appearance on MEA (Fig. 2a), with white mycelia growing superficially on the agar. The optimal temperature for growth was 30 °C, reaching 79.0 mm in diam in 6 days. Slow growth at 35 °C. No growth was observed at 5 °C.

Description. *Hyphae* white, growing radially with branching and septation (Fig. 2b); *conidiophores*, directly arising singly from the vegetative hyphae, measuring (54.3 –) 68.7 – 130.7 (– 166.5) × (1.2 –) 1.8 – 2.8 (– 3.7) μm (Fig. 2c – e); *conidia* hyaline to subhyaline, uni-septate, smooth, ellipsoidal, with sizes of (7.7-) 9.1 – 12.7 (– 16.9) × (2.5 –) 3.1 – 4.3 (– 4.9) μm, apex obtuse, gradually tapering towards the base (Fig. 2b, e). The fungus captures nematodes using adhesive networks that are formed 36 h after exposure to the host (Fig. 2f, g). Sexual morph is unknown.

Note. *Arthrobotrys byssisimilis* is closely related to *A. dendroides* and *A. anomalus* but forms a distinct clade in the concatenated ITS, EF, and RPB2 phylogenetic tree (Fig. 1). It differs from *A. anomalus* by 46 ITS base pairs and from *A. dendroides* by 62. The EF gene shows 62 base pair differences from both species, while RPB2 differs by 141 base pairs from *A. anomalus* and 157 from *A. dendroides*.

Morphologically, *A. byssisimilis* has exclusively mononematous conidiophores, whereas *A. dendroides* predominantly forms synnematous ones. Its conidiophores are shorter than those of *A. dendroides* (166.5 μm vs. 800 μm) (Kuthubutheen et al., 1985) but longer than those of *A. anomalus* (166.5 μm vs. 80 μm) (Barron and Davidson 1972). The conidia resemble those of both species but are shorter than those of *A. dendroides* (16.9 μm vs. 22 μm) and thinner than those of *A. anomalus* (4.9 μm vs. 8.5 μm). Additionally, *A. byssisimilis* conidia develop a septum upon attachment to the conidiophores, while *A. anomalus* forms a septum before germination.

3.3. Chitinase and protease activity assay

Chitinase activity in *A. byssisimilis* increased initially but declined with rising temperature, while protease activity consistently increased (Fig. 3a). The optimal temperatures were 25 °C for chitinase and 55 °C for protease. Chitinase activity increased with pH, whereas protease activity peaked before declining. The optimal pH was 10 for chitinase and 8 for protease (Fig. 3b).

3.4. Nematicidal activity of liquid fungal culture filtrate

When conducting nematicidal activity assays using the liquid fungal culture filtrate, *A. byssisimilis* exhibited 100 % nematicidal activity within approximately 10 min at full strength (100 % concentration). When diluted to 50 %, complete nematode mortality was achieved in 30 min. At dilutions of 25 % or lower, the mortality rate of nematodes ranged from 60–80 % within the same time frame (Fig. 3c).

3.5. Nematicidal activity assay of protein concentrate

The undiluted protein concentrate of *A. byssisimilis* achieved 100 % nematode mortality within 30 min. At a 50 % dilution, the mortality rate decreased to 60 % over the same period. For dilutions of 25 % or lower, the nematode mortality rate ranged between 20 % and 60 % within 30 min (Fig. 3d).

3.6. Nematicidal activity assay of secondary metabolites

The secondary metabolite extracts of *A. byssisimilis* induced 100 % nematode mortality within 15 min at concentrations ranging from 100 % to 25 %. At a 6.25 % concentration, the mortality rate reaches nearly 60 % after 15 min and 100 % after 30 min (Fig. 3e).

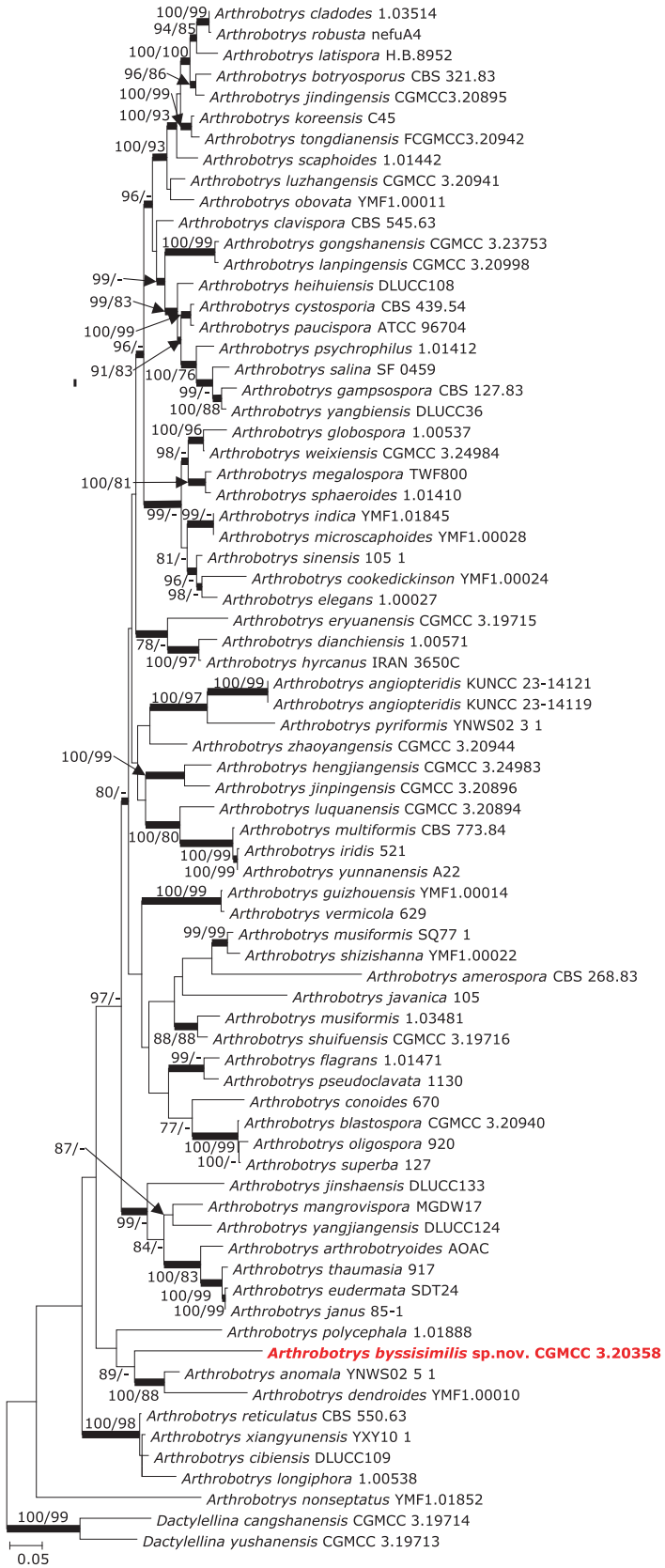

Fig. 1. Maximum likelihood tree of *Arthrobotrys* species constructed using the concatenated dataset (ITS + EF + RPB2). Bootstrap support values ≥ 75 % are indicated above the nodes as ML/MP, and posterior probabilities ≥ 0.90 are indicated by bold branches. Isolates obtained in this study are in bold font.

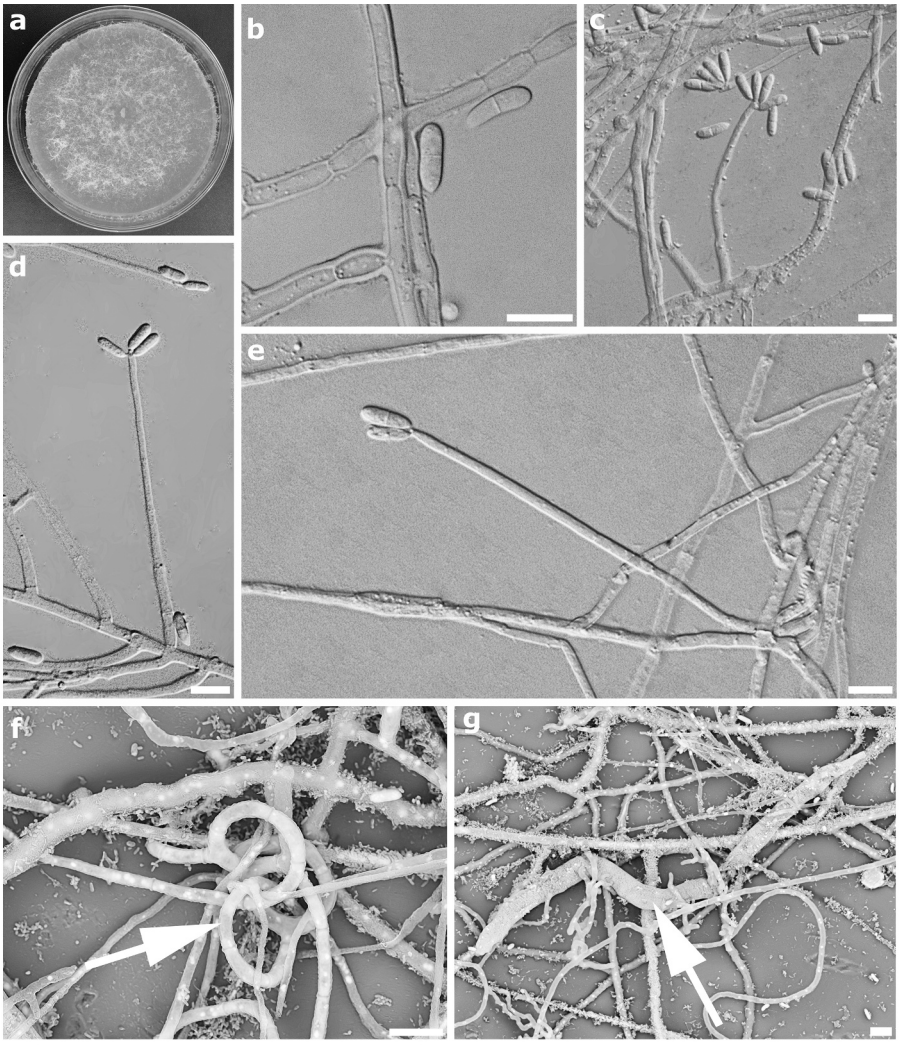

Fig. 2. Morphology of *Arthrobotrys byssisimilis* sp. nov. (HMAS 352341) **a** top view of 10-day-old culture growing on a MEA; **b** hyphae; **c**–**e** conidiophore with conidia; **f** SEM view of trapping net, indicated by the arrow**; r** SEM view of nematode trapped by net, with the nematode highlighted by the arrow. Scale bars = 5 μm.

3.7. Assessment of fungal growth in the presence of antimicrobials

Ethanol concentrations of 0.5 % and 1 % did not affect the hyphal growth of *A. byssisimilis*, but concentrations above 1 % led to inhibition, with almost complete cessation of growth at 5 % (Fig. 3f). The fungal growth was not significantly affected by α-pinene at a volume of less than or equal to 5 μL. However, hyphal growth was noticeably inhibited when the amount exceeded 50 μL. For β-pinene, no significant difference was noted at 0.5 μL, but hyphal growth was inhibited at higher amounts, with nearly complete arrest of hyphal growth at 500 μL. Similarly, oleum terebinthinae has no significant effect below 50 μL, but at 500 μL, significant inhibition of hyphal growth was observed.

3.8. Whole genome sequencing, assembly and annotation

The *A. byssisimilis* genome assembly (JBMHBI000000000) consists of 231 scaffolds, with an N50 of 1,449,140 bp and an estimated genome size of 36.97 Mb. The GC content is 46.06 %, and BUSCO analysis indicates 99.0 % completeness (Table S1).

Repeat annotation using RepeatMasker classified 0.35 % of the genome as repetitive, mainly comprising long terminal repeats (LTRs) (0.14 %) and DNA transposons (0.11 %) (Table S2). However, de novo annotation with RepeatModeler identified a higher proportion of repetitive sequences (1.74 %), with LTRs contributing 1.08 % (Table S3).

The assembly contains 8,354 predicted ORFs, with an average gene length of 1,695.4 bp. Coding sequences span approximately 14.2 Mb (38.31 % of the genome), with 27,169 exons covering 12.7 Mb (34.40 %). Functional annotation identified 109 tRNAs, six rRNAs (one 5.8S, three 18S, and two 28S), and 25 additional non-coding RNAs (Table S4).

CAZyme analysis revealed 433 carbohydrate-active enzymes, predominantly glycoside hydrolases (178 genes), with carbohydrate-binding modules being the least abundant (16 genes; Fig. 4a). Antibiotic resistance and biosynthesis annotation identified three resistance genes and one biosynthesis gene. BLAST searches against the DFVF database detected 899 fungal virulence factors and 795 predicted secreted proteins.

Gene function annotation using NCBI-nr and Swiss-Prot databases assigned functions to 8,012 and 5,536 genes, respectively (Table S5). eggNOG-mapper classified 6,283 genes into 25 functional categories, with the largest groups involved in post-translational modification (490 genes) and carbohydrate metabolism (440 genes). The least represented categories included nuclear structure (3 genes) and extracellular structures (4 genes; Fig. 4b).

The fungal cytochrome P450 database identified 4,076 genes with > 30 % sequence similarity, of which 218 exhibited > 50 % similarity. Transporter classification revealed 1,315 transport-related genes, predominantly electrochemical potential-driven transporters (333 genes), with the fewest classified as transmembrane electron carriers (13 genes;

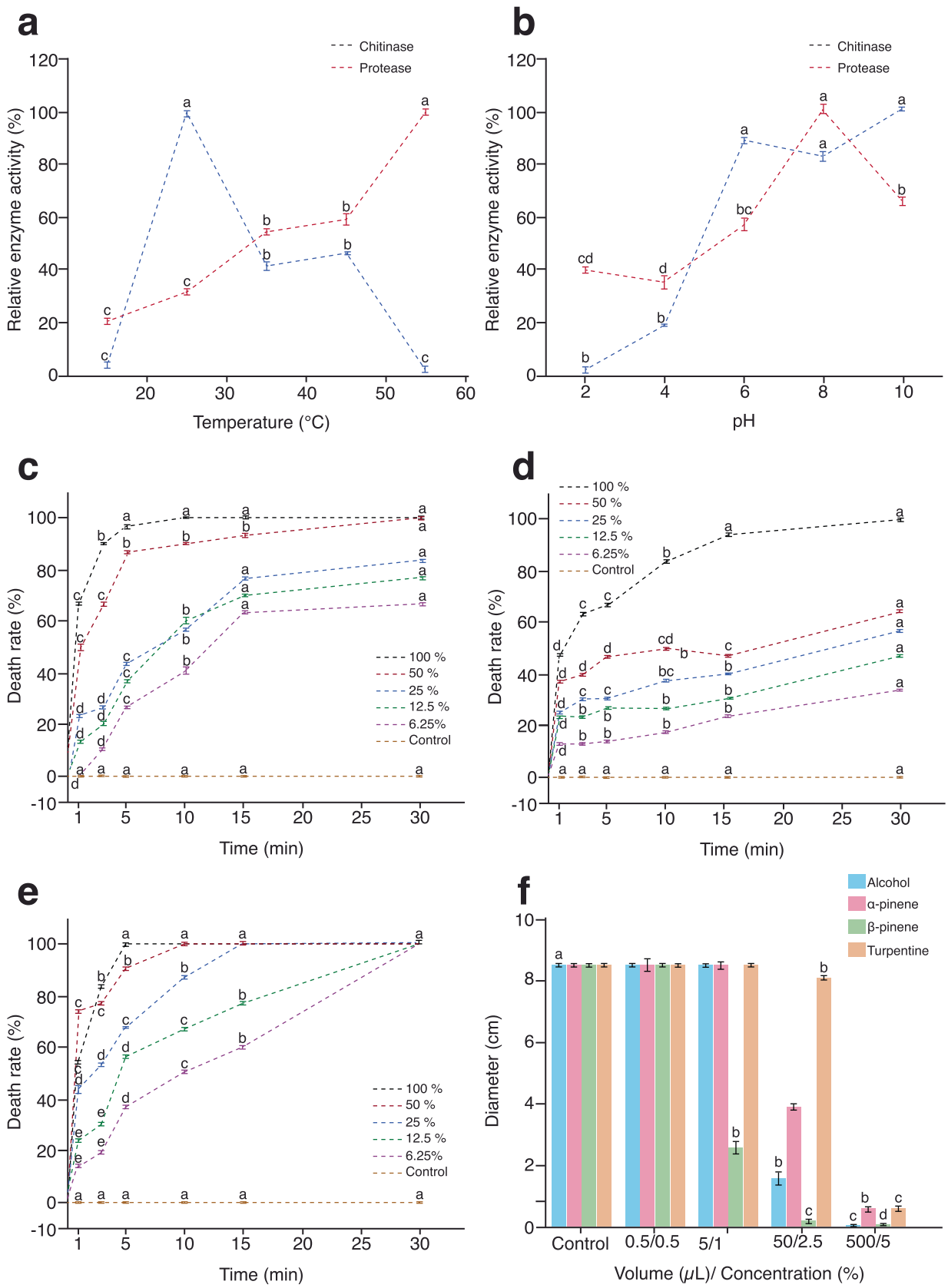

Fig. 3. The effect of temperature and pH on the activity of chitinase and protease, the nematicidal activity of liquid culture filtrate, protein concentrate, and secondary metabolite, and the effect of defending compounds on the growth of *Arthrobotrys byssisimilis*. **a** the effect of temperature on the activity of chitinase and protease; **b** the effect of pH on the activity of chitinase and protease; **c** the nematicidal activity of different dilutes of liquid culture filtrate; **d** the nematicidal activity of different dilutes of protein concentrate; **e** the nematicidal activity of different dilutes of secondary metabolite; **f** the effect of α-pinene, β-pinene, oleum terebinthinae and ethanol on the growth of *Arthrobotrys byssisimilis*.

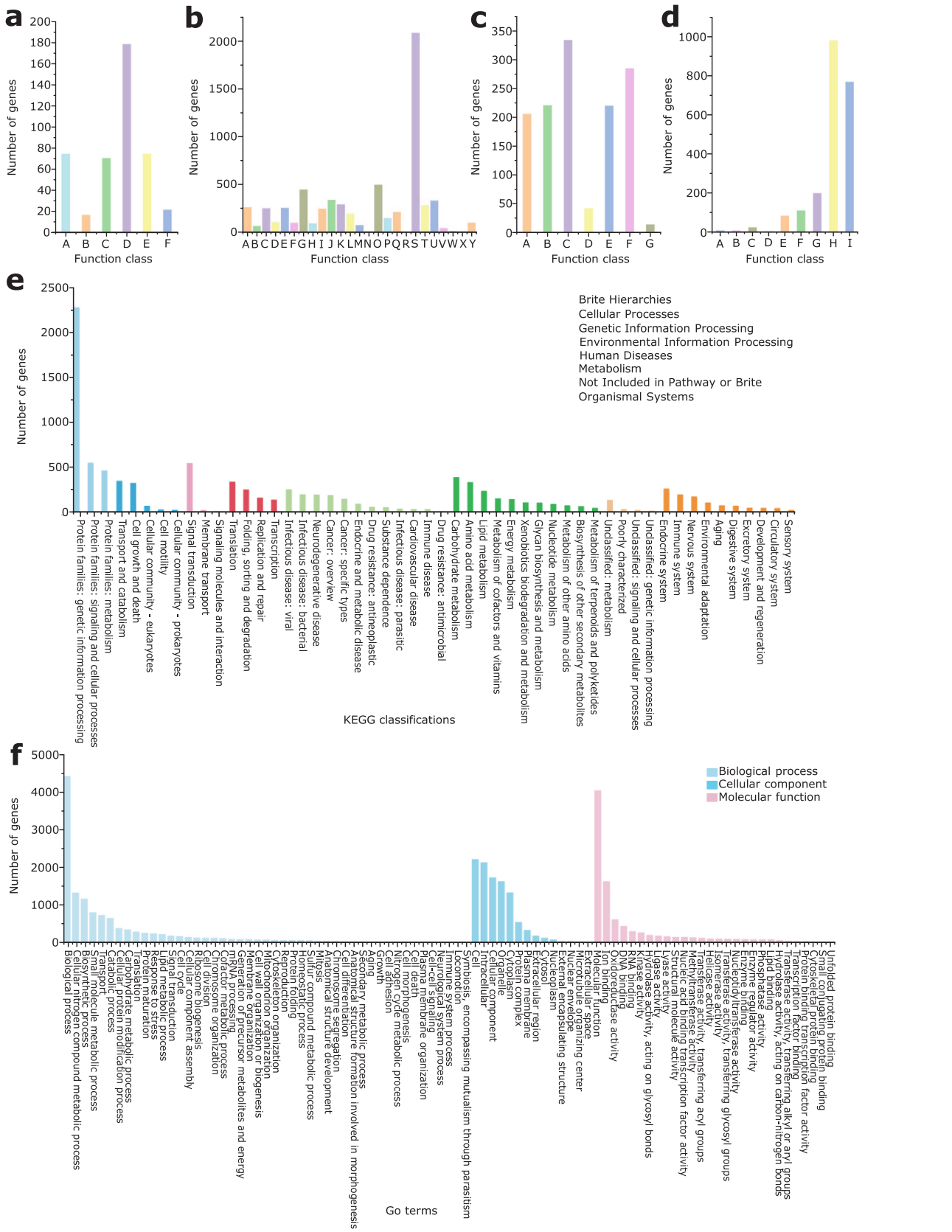

(caption on next page)

Fig. 4. Carbohydrate-active enzymes (CAZymes) identification and gene functional annotation of *Arthrobotrys byssisimilis*. **a:** CAZymes identified in the genome which were divided into six functional classes. These were Glycosyl Transferases (GT), Polysaccharide Lyases (PL), Carbohydrate Esterases (CE), Auxiliary Activities (AA), Carbohydrate-Binding Modules (CMB), and Glycoside Hydrolases (GH); **b:** eggNOG classifications of assembled unigenes. The functional annotations were divided into 25 categories, corresponding to clusters of orthologous groups (COGs). A = RNA processing and modification, B = Chromatin structure and dynamics, C = Energy production and conversion, D = Cell cycle control, cell division, chromosome partitioning, E = Amino acid transport and metabolism, F = Nucleotide transport and metabolism, G = Carbohydrate transport and metabolism, H = Coenzyme transport and metabolism, I = Lipid transport and metabolism, J = Translation, ribosomal structure and biogenesis, K = Transcription, L = Replication, recombination and repair, M = Cell wall/membrane/envelope biogenesis, N = Cell motility, O = Posttranslational modification, protein turnover, chaperones, P = Inorganic ion transport and metabolism, Q = Secondary metabolites biosynthesis, transport and catabolism, R = General function prediction only, S = Function unknown, T = Signal transduction mechanisms, U = Intracellular trafficking, secretion, and vesicular transport, V = Defense mechanisms, W = Extracellular structures, X = Nuclear structure, Y = Cytoskeleton; **c:** Transport proteins annotation of assembled unigenes. Unigenes were summarized into seven main categories. A = Channels/Pores, B = Electrochemical Potential-driven Transporters, C = Primary Active Transporters, D = Group Translocators, E = Transmembrane Electron Carriers, F = Accessory Factors Involved in Transport, G = Incompletely Characterized Transport Systems; **d:** Pathogen-host interactions (PHI) annotation of assembled unigenes. Unigenes were summarized into nine main categories. A = Chemistry target: resistance to chemical, B = Chemistry target: sensitivity to chemical, C = Effector (plant avirulence determinant), D = Enhanced antagonism, E = Increased virulence (hypervirulence), F = Lethal, G = Loss of pathogenicity, H = Reduced virulence, I = Unaffected pathogenicity; **e:** Kyoto Encyclopedia of Genes and Genomes (KEGG) Orthology annotation of assembled unigenes. The unigenes were summarized into eight main categories; **f:** Gene ontology (GO) classification of assembled unigenes. Unigenes were summarized into three main categories.

Fig. 4c).

The Pathogen-Host Interactions (PHI) database predicted 1929 genes involved in host interactions, with most linked to loss of pathogenicity (196 genes), reduced virulence (978 genes), or unaffected pathogenicity (766 genes; Fig. 4d). KEGG annotation assigned 3405 genes to metabolic and cellular pathways, including 1678 genes in metabolism and 1222 in human disease-related pathways (Fig. 4e). InterPro classified 12,609 genes into biological processes, cellular components (10,309 genes), and molecular functions (9153 genes), with 17 genes involved in secondary metabolism (Fig. 4f).

We identified 104 protease-encoding genes, classified as aspartic (12 genes), cysteine (3), metalloproteases (27), and serine proteases (62). Among them, 41 contain signal peptides, and 32 are secretory proteins. Additional enzymatic genes include eight chitinases, three cellulases, four cellobiohydrolases, four pectinesterases, seven lectins, 32 lipases, and four cutinases, many of which may contribute to pathogenicity.

Using antiSMASH, we detected 21 core biosynthetic genes, including seven Type I Polyketide Synthases (T1PKSs), one Type III PKS (T3PKS), six terpenes, two Non-Ribosomal Peptide Synthetases (NRPSs), and other biosynthetic pathways. Additionally, 19 accessory biosynthetic genes, one regulatory gene, and one transport-related gene were identified.

3.9. Transcriptome sequencing and analyses

Following data processing, we obtained a total of 270.82 million clean reads. Each sample yielded more than 6.15 Gb of clean bases, with Q20 values exceeding 98.38 % and Q30 values above 94.91 %, ensuring high sequencing quality. Alignment rates with the reference genome ranged from 90.93 % to 95.56 %, with unique mapping rates above 90.61 % (Table S6), confirming the suitability of the data for downstream analyses. Raw transcriptomic data are available under NCBI BioProject PRJNA1236497 (SRA accessions: SRR33132835-SRR33132839).

Principal component analysis (PCA) revealed clear distinctions in gene expression between nematode-induced and control groups, highlighting strong biological reproducibility (Fig. 5a). Differential expression analysis identified 638 differentially expressed genes (DEGs), with 394 upregulated and 244 downregulated. Hierarchical clustering further demonstrated a distinct separation between treatment groups based on gene expression patterns (Fig. 5b). Gene Ontology (GO) enrichment analysis of the top 20 GO terms indicated significant associations with response to stress (GO:0006950), transporter activity (GO:0005215), and nucleobase-containing small molecule metabolic processes (GO:0055086) (Fig. 5c). Kyoto Encyclopedia of Genes and Genomes (KEGG) pathway enrichment analysis highlighted starch and sucrose metabolism, Huntington's disease, and ribosome pathways among the top 20 enriched pathways (Fig. 5d).

Further analyses focused on key functional gene categories, including enzymes, polyketide synthases (PKSs), cytochrome P450 monooxygenases (P450s), pathogen-host interaction (PHI) genes, and fungal virulence factor genes (Fig. 6). Among the 32 lipase genes, three were upregulated, while one of the three cellulase genes was also upregulated. Differential expression was observed in protease families: two serine protease genes were upregulated, and one was downregulated among 63 identified genes; two metalloprotease genes were upregulated, and two were downregulated among 27 genes; and one of 12 aspartic protease genes was upregulated. In the chitinase gene family, one of the eight genes was downregulated.

Among PKS genes, four of the 19 additional biosynthetic genes were upregulated, while one of the 21 core biosynthetic genes was downregulated. Of the 218 P450 genes (with identity > 50 % against the P450 database), 13 were upregulated and five were downregulated. Within the 1,929 PHI genes, 70 were upregulated and 61 were downregulated. Carbohydrate-active enzymes (CAZymes) analysis revealed that 11 genes were upregulated, including one Glycosyl Transferase, one Polysaccharide Lyase, three Carbohydrate Esterases, two Auxiliary Activities, and four Glycoside Hydrolases. Meanwhile, 16 CAZyme genes were downregulated, comprising two Glycosyl Transferases, two Carbohydrate Esterases, one Auxiliary Activity, and 11 Glycoside Hydrolases. No antibiotic-related genes exhibited differential expression. Finally, among the 899 fungal virulence factors, 34 were upregulated and 32 were downregulated, suggesting potential implications for nematode-pathogen interactions.

4. Discussion

During a survey of bark beetle-associated fungi, *Arthrobotrys byssisimilis* sp. nov. was isolated from a *Pinus thunbergii* gallery and identified as a new species through multi-locus phylogenetic analysis (ITS, TEF1-α, and RPB2). Morphological novelty and genetic divergence from its closest relatives, *A. dendroides* and *A. anomala*, further supported its taxonomic status. *Arthrobotrys byssisimilis* demonstrated potent nematicidal activity against PWN, achieving 100 % mortality within 10–30 min, depending on the treatment type, culture filtrate, protein concentrate, or secondary metabolites. The fungus produced chitinase and protease enzymes with distinct temperature and pH optima and showed tolerance to several pine-derived antimicrobial compounds. Genome sequencing revealed a 36.97 Mb genome encoding 8,354 predicted proteins, including numerous genes linked to pathogenicity, enzyme production, and secondary metabolism. Transcriptomic analysis during nematode interaction identified 638 differentially expressed genes, underscoring its potential as a biocontrol agent.

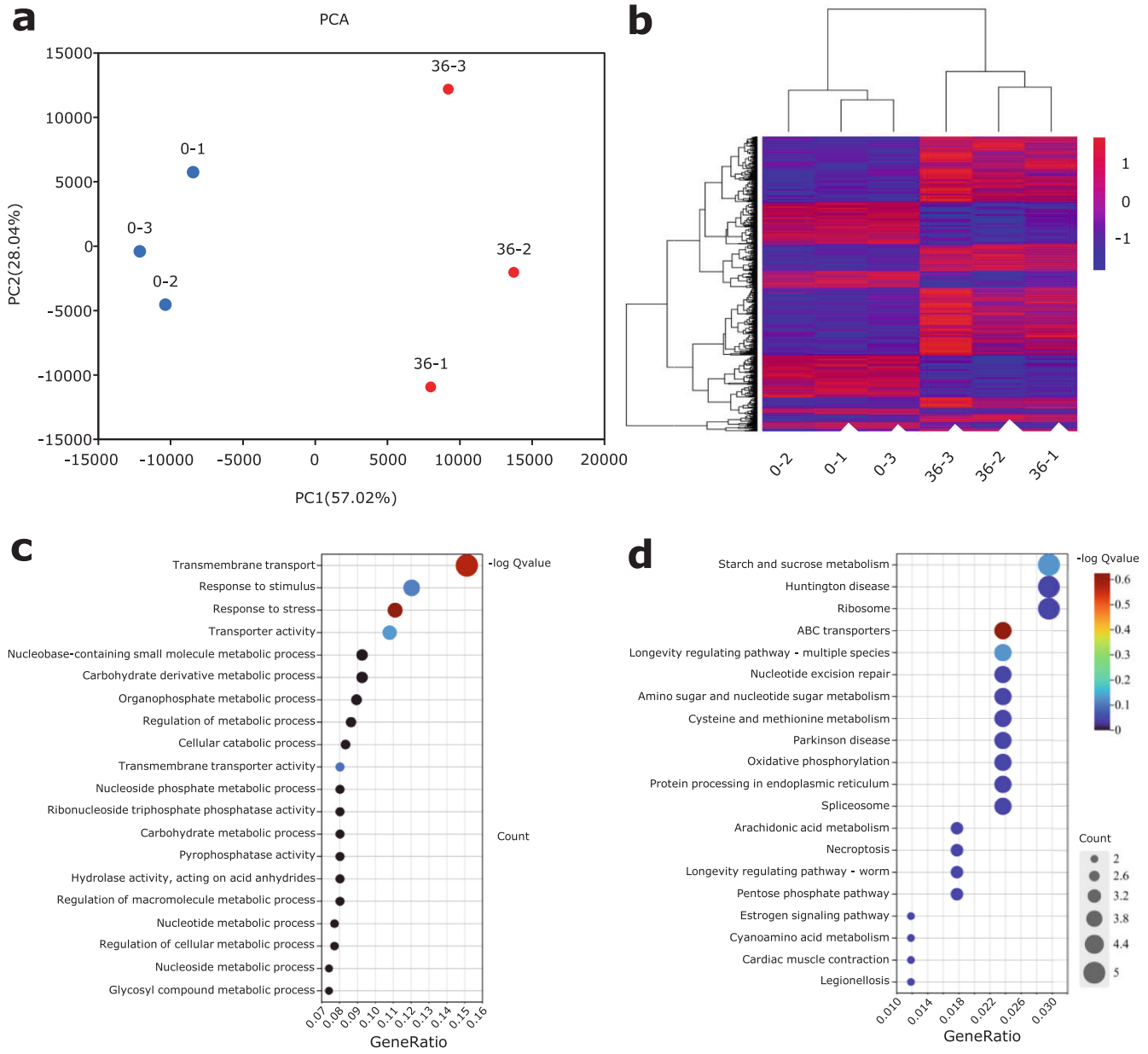

Fig. 5. Transcriptomic analysis of *Arthrobotrys byssimilis* under nematode infection. **a** Principal Component Analysis (PCA) showing the distribution of samples based on gene expression profiles. Blue and red dots represent samples not induced and induced by *Bursaphelenchus xylophilus*; **b** Hierarchical clustering analysis of DEGs, illustrating the expression patterns across samples induced and not induced by *Bursaphelenchus xylophilus*; **c** The top 20 significantly enriched Gene Ontology (GO) terms based on DEGs; **d** Top 20 significantly enriched Gene Ontology (GO) terms. (For interpretation of the references to color in this figure legend, the reader is referred to the web version of this article.)

4.1. Characterizing a novel Arthrobotrys from the bark beetle gallery

We isolated and classified a novel *Arthrobotrys* species, *A. byssisimilis,* from a bark beetle gallery. *Arthrobotrys* species are widely distributed across various habitats, including farmlands, forests, heavy metal-contaminated areas, and sediments from marine, freshwater, and hot spring environments, due to their unique survival strategies (Zhang et al., 2024a). Various nematodes are often found associated with bark beetles (Hussain et al., 2022; Resnerová et al., 2022; Ryss and Subbotin 2023); however, the presence of *Arthrobotrys* in bark beetle-associated environments was previously undocumented. This finding extends the known ecological range of *Arthrobotrys* and underscores its remarkable adaptability.

Currently, the taxonomy of the genus *Arthrobotrys* primarily relies on the analysis of ITS, EF, and RPB2 gene regions (Zhang et al., 2023a; Zhang et al., 2023b). However, in this study, we could not amplify the RPB2 gene of *A. byssisimilis* using the primer pair RPB2-6F/RPB2-7R, which has been used in previous research (Zhang et al., 2022a; Zhang et al., 2023a; Zhang et al., 2023b, 2024a). Consequently, the RPB2 sequence was extracted directly from the genome sequence. Upon comparing our sequence with the primers, mismatches were identified as follows:

RPB2-6F: tgg gg(**G**/**T**) (t/a)tg gt(c/t)tg(t/c)cc**T** gc vs. tgg gg**C** ttg gtc tgc cc**C** gc.

RPB2-7R: ccc at(a/t) gc(c/t) tg**C** tt(c/a)ccc at vs. ccc ata gct tg**T** tta ccc at.

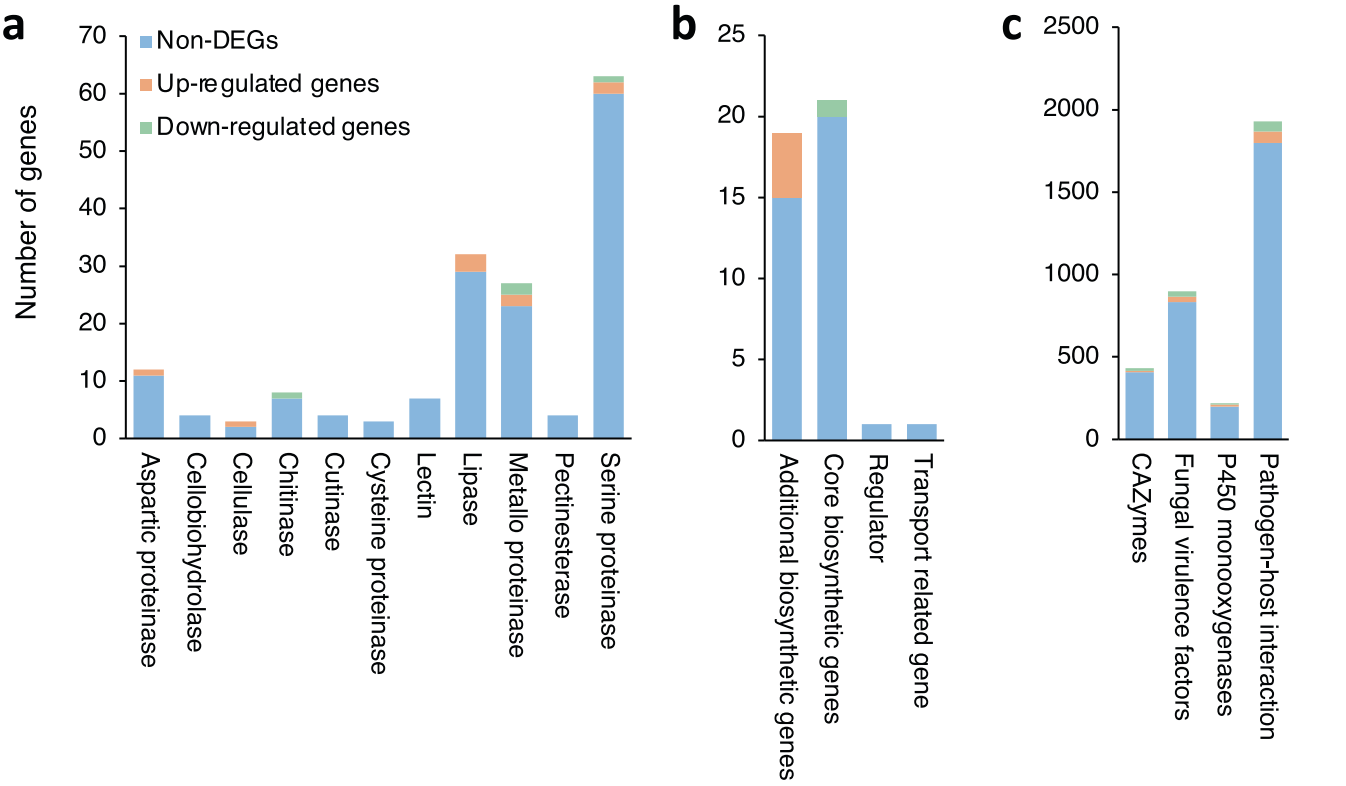

Fig. 6. Differentially expressed genes related to the pathogenicity of *Arthrobotrys byssimilis* towards *Bursaphelenchus xylophilus*. **a** enzymes; **b** polyketide synthases; **c** cytochrome P450 monooxygenases, pathogen-host interaction genes, and a database of fungal virulence factors genes in the genome.

These mismatches likely account for the amplification failure and highlight the limitations of current RPB2 primers in detecting genetic diversity within *Arthrobotrys*. Future studies should prioritize the development of more broadly compatible primers or employ genome-guided approaches to ensure reliable amplification across diverse species within the genus.

4.2. Nematicidal mechanisms and biocontrol potential of *A. byssisimilis*

Arthrobotrys byssisimilis exhibited strong nematicidal activity, with 100 % mortality of PWN achieved within 10 min by liquid culture filtrate, 30 min by protein-enriched fractions, and 15 min by secondary metabolites. The superior efficacy of the culture filtrate likely results from the synergistic action of enzymes and secondary metabolites. Compared to other *Arthrobotrys* species, which often show much lower nematode mortality rates under similar conditions, *A. byssisimilis* demonstrates exceptional biocontrol potential. For instance, *A. shizishananus* achieved only 30 % mortality against *Panagrellus redivivus* over 30 h, while *A. conoides* and *A. oligospora* reached less than 30 % mortality against *Meloidogyne* spp. even after 24 h of exposure (Nourani et al., 2015; Wang et al., 2006b).

Protease and chitinase activities were detected in the liquid culture, each showing distinct pH and temperature optima. The protease activity profile (optimal at 55 °C and pH 8.5) differed from that of known virulence factors like Aoz1 (optimal at 45 °C and pH 6–8) (Zhao et al., 2004), and no PII homologs were found in the genome. This suggests the involvement of novel protease families, supported by the identification of 104 putative protease-encoding genes. Similarly, multiple chitinase genes were annotated, although their specific roles in nematode predation remain to be determined. These findings warrant further investigation through gene knockout and enzyme purification to identify key effector proteins responsible for nematode killing.

To assess host colonization potential, the growth of *A. byssisimilis* was tested in the presence of compounds commonly found in pine trees, including α-pinene, β-pinene, oleum terebinthinae, and ethanol. No significant inhibition was observed at concentrations ≤ 5 μL for terpenes or ≤ 1 % for ethanol. Unlike many fungal symbionts of bark beetles that are inhibited by ethanol (Lehenberger et al., 2021), *A. byssisimilis* maintained robust growth, indicating its capacity to tolerate host-associated antimicrobial compounds. Although no growth-promoting effect of low α-pinene concentrations was observed, the fungus remained unaffected, suggesting it can persist in host environments conducive to nematode infection.

The demonstrated in vitro nematicidal efficacy and pine volatile tolerance position *A. byssimilis* as a promising biocontrol agent for pine wilt disease, particularly in high-risk zones where chemical control is restricted. However, the field efficacy of *A. byssimilis* may be challenged by multiple factors, such as environmental variability, delivery method limitations, and ecological interactions. Furthermore, regulatory approval requires comprehensive ecotoxicological assessments, particularly regarding non-target effects on beneficial nematodes. While showing strong activity against *B. xylophilus*, the effectiveness of this strain against other economically important phytoparasitic nematodes remains unknown. Given that fungal strains often exhibit species-specific efficacy (Kassam et al., 2021; Nourani et al., 2015; Wu et al., 2023), broader screening is essential to determine their applicability across diverse nematode targets and to identify optimal strain–nematode pairings for biocontrol.

4.3. Multi-omics profiling reveals nematocidal mechanisms in *Arthrobotrys byssisimilis*

The genome of *A. byssisimilis* is 36.97 Mb, which is smaller than most *Arthrobotrys* species except *A. flagrans* (36.32 Mb), and contains 8,354 predicted open reading frames (ORFs), fewer than the 11,479 ORFs reported in *A. oligospora* (Yang et al., 2011; Zhang et al., 2024c). Due to limited annotation data for other species, further comparative analysis is currently constrained.

Genome annotation revealed a broad array of genes potentially involved in nematode predation, including 104 proteases, 8 chitinases, 3 cellulases, 4 cellobiohydrolases, 4 pectinesterases, 7 lectins, 32 lipases, and 4 cutinases. However, many of these are not predicted to be secreted. For example, of the eight chitinase genes identified, only three encode secretory proteins. Two chitinase homologs, *scaffold7.t258* and *scaffold12.g147*, related to nematocidal genes *AOL_379* and *AOL_483* (Gong et al., 2022; Gong et al., 2019; Zhang et al., 2024b; Zhong et al., 2019), lack signal peptides and transmembrane domains, suggesting they are intracellular. How these proteins contribute to nematode killing remains unclear.

Secondary metabolites also play a key role in nematode suppression. Biosynthetic gene cluster analysis using antiSMASH identified 8 polyketide synthases (PKSs), more than the 5 reported for *A. oligospora* (Yang et al., 2011). To standardize comparisons, we re-analyzed the *A. oligospora* genome using the same antiSMASH version, revealing 13 core biosynthetic genes, still fewer than the 21 found in *A. byssisimilis*. The functional relevance of this difference remains to be established. Similarly, *A. byssisimilis* harbors significantly more cytochrome P450 monooxygenases (P450s) than *A. oligospora*, though this may reflect database differences or true species-level variation. Notably, the number of fungal P450s cataloged in public databases has expanded substantially over the past decade, complicating direct comparisons.

Transcriptome analysis during nematode interaction showed limited differential expression of protease and chitinase genes, with even fewer differentially expressed secretory proteins. Among 62 serine protease genes, 20 encode predicted secretory proteins, yet none were differentially expressed. This lack of expression change may be due to the specific time point chosen for sampling. Prior studies have shown stage-specific expression of key virulence genes—for instance, chitinase *AO-379* in *A. oligospora* (homologous to *scaffold7.t258*) is differentially expressed at distinct trapping stages (Jia et al., 2023). Likewise, no core secondary metabolite biosynthetic genes were upregulated, and only 13 P450s with $\geq$ 50 % identity to known P450s showed differential expression.

These findings suggest that nematocidal gene expression in *A. byssisimilis* is likely dynamic and time-dependent. Future studies should incorporate multiple time points and functional assays to fully elucidate the regulatory networks driving enzyme and metabolite-mediated nematode killing.

5. Conclusions

The identification of *A. byssisimilis* adds to the known diversity of nematode-trapping fungi and highlights novel genetic features, including unique proteases, chitinases, and secondary metabolite biosynthetic genes. Its high nematicidal activity, despite lacking known virulence factors like PII, suggests alternative and efficient mechanisms of nematode killing. Ecologically, this is the first *Arthrobotrys* species found in a bark beetle gallery, indicating a broader habitat range and potential involvement in bark beetle–nematode interactions. Its tolerance to pine-derived compounds like α-pinene and ethanol further supports its adaptability to forest environments. Functionally, *A. byssisimilis* achieved 100 % mortality of *Bursaphelenchus xylophilus* within minutes, outperforming other known nematophagous fungi. However, commercial development of *A. byssimilis* requires method optimization for field delivery, scalable production protocols, and thorough environmental safety testing. Parallel investigation of its effectiveness against other nematodes and effector genes will further enable targeted strain improvement.

CRediT authorship contribution statement

Mengting Gao: Methodology, Investigation, Formal analysis. **Zhaoqi Yan:** Methodology, Formal analysis, Data curation. **Zexin Liu:** Formal analysis, Data curation. **Yunxia Jiang:** Methodology, Data curation. **Tengteng Liu:** Resources. **Xingjun Miao:** Resources. **Meixue Dai:** Supervision, Methodology, Investigation, Conceptualization. **Tanay Bose:** Writing – review & editing, Writing – original draft, Formal analysis, Data curation. **Runlei Chang:** Writing – review & editing, Writing – original draft, Supervision, Methodology, Investigation, Funding acquisition, Formal analysis, Data curation, Conceptualization.

Funding

This work was also supported by the Natural Science Foundation of Shandong Province [Grant No. ZR2024MC133].

Declaration of competing interest

The authors declare that they have no known competing financial interests or personal relationships that could have appeared to influence the work reported in this paper.

Acknowledgement

The authors would like to thank Prof. Xudong Zhou of the Zhejiang A&F University for providing isolates of *Bursaphelenchus xylophilus*.

Appendix A. Supplementary data

Supplementary data to this article can be found online at https://doi.org/10.1016/j.biocontrol.2025.105853.

References

Ahman, J., Ek, B., Rask, L., Tunlid, A., 1996. Sequence analysis and regulation of a gene encoding a cuticle-degrading serine protease from the nematophagous fungus *Arthrobotrys oligospora*. Microbiology 142, 1605–1616. https://doi.org/10.1099/13500872-142-7-1605.

Almagro Armenteros, J.J., Tsirigos, K.D., Sønderby, C.K., Petersen, T.N., Winther, O., Brunak, S., von Heijne, G., Nielsen, H., 2019. SignalP 5.0 improves signal peptide predictions using deep neural networks. Nat. Biotechnol. 37, 420–423. https://doi.org/10.1038/s41587-019-0036-z.

Altschul, S.F., Gish, W., Miller, W., Myers, E.W., Lipman, D.J., 1990. Basic local alignment search tool. J. Mol. Biol. 215, 403–410. https://doi.org/10.1016/s0022-2836(05)80360-2.

Anders, S., Pyl, P.T., Huber, W., 2015. HTSeq—a Python framework to work with high-throughput sequencing data. Bioinformatics 31, 166–169. https://doi.org/10.1093/bioinformatics/btu638.

Back, M.A., Bonifácio, L., Inácio, M.L., Mota, M., Boa, E., 2024. Pine wilt disease: a global threat to forestry. Plant Pathol. 73, 1026–1041. https://doi.org/10.1111/ppa.13875.

Bahena-Nuñez, D.S., Ocampo-Gutiérrez, A.Y., Mendoza-de Gives, P., González-Cortázar, M., Zamilpa, A., Higuera-Piedrahita, R.I., Pérez-Anzúrez, G., Olmedo-Juárez, A., López-Arellano, M.E., Delgado-Núñez, E.J., Hernández-Romano, J., 2024. *Arthrobotrys oligospora* (Fungi: Orbiliales) and its liquid culture filtrate myco-constituents kill *Haemonchus contortus* infective larvae (Nematoda: trichostrongylidae). Biocontrol Sci. Tech. 34, 754–775. https://doi.org/10.1080/09583157.2024.2377607.

Bankevich, A., Nurk, S., Antipov, D., Gurevich, A.A., Dvorkin, M., Kulikov, A.S., Lesin, V. M., Nikolenko, S.I., Pham, S., Prjibelski, A.D., Pyshkin, A.V., Sirotkin, A.V., Vyahhi, N., Tesler, G., Alekseyev, M.A., Pevzner, P.A., 2012. SPAdes: a new genome assembly algorithm and its applications to single-cell sequencing. J. Comput. Biol. 19, 455–477. https://doi.org/10.1089/cmb.2012.0021.

Bao, Z., Eddy, S.R., 2002. Automated de novo identification of repeat sequence families in sequenced genomes. Genome Res. 12, 1269–1276. https://doi.org/10.1101/gr.88502.

Barron, G.L., Davidson, J.G.N., 1972. Nematophagous Hyphomycetes: *Arthrobotrys anomala* sp. nov. Can. J. Bot. 50, 1773–1774. https://doi.org/10.1139/b72-220.

Blin, K., Shaw, S., Augustijn, H.E., Reitz, Z.L., Biermann, F., Alanjary, M., Fetter, A., Terlouw, B.R., Metcalf, W.W., Helfrich, E.J.N., van Wezel, G.P., Medema, M.H., Weber, T., 2023. antiSMASH 7.0: new and improved predictions for detection, regulation, chemical structures and visualisation. Nucleic Acids Res. 51, W46–W50. https://doi.org/10.1093/nar/gkad344.

Buchfink, B., Xie, C., Huson, D.H., 2015. Fast and sensitive protein alignment using DIAMOND. Nat. Methods 12, 59–60. https://doi.org/10.1038/nmeth.3176.

Cayrol, J. C., 1983. Lutte biologique contre les Meloidogyne au moyen d'*Arthrobotrys irregularis*. pp. 265–273.

Cayrol, J.C., Frankowski, J.P., Laniece, A., D'Hardemare, G., Talon, J.P., 1978. Contre les nematodes en champignoniere. Mise au point d'une methode de lutte biologique a l'aide d'un hypomicete predateur: Arthrobotrys robusta souche antipolis (Royal 300). Revue Horticole. 184, 23–30.

Chen, J., Jiao, N., Ran, Y., Wu, Z., Pan, J., Lu, X., Hao, X., 2024. Assessing effect of *Trichoderma asperellum* T16 on management of *Bursaphelenchus xylophilus*. Ind. Crop. Prod. 215, 118628. https://doi.org/10.1016/j.indcrop.2024.118628.

Chen, Y.-H., Liu, X., Dai, R., Ou, X., Xu, Z.-F., Zhang, K.-Q., Niu, X.-M., 2020. Novel polyketide-terpenoid hybrid metabolites and increased fungal nematocidal ability by disruption of genes 277 and 279 in nematode-trapping fungus *Arthrobotrys oligospora*. J. Agric. Food Chem. 68, 7870–7879. https://doi.org/10.1021/acs.jafc.0c01720.

Chen, Y.H., Zhang, L.L., Wang, L.J., Yue, X.T., Wu, Q.F., Jiang, Y., Zhang, K.Q., Niu, X. M., 2022. Acetylation of sesquiterpenyl epoxy-cyclohexenoids regulates fungal growth, stress resistance, endocytosis, and pathogenicity of nematode-trapping fungus *Arthrobotrys oligospora* via metabolism and transcription. J. Agric. Food Chem. 70, 6145–6155. https://doi.org/10.1021/acs.jafc.2c01914.

Coil, D., Jospin, G., Darling, A.E., 2014. A5-miseq: an updated pipeline to assemble microbial genomes from Illumina MiSeq data. Bioinformatics 31, 587–589. https://doi.org/10.1093/bioinformatics/btu661.

Corda, A.C.J., 1839. Pracht-flora europaeischer schimmelbildungen. Ann. Mag. Nat. Hist. 4, 200–201. https://doi.org/10.1080/00222933909512494.

Darriba, D., Taboada, G.L., Doallo, R., Posada, D., 2012. jModelTest 2: more models, new heuristics and parallel computing. Nat. Methods 9, 772. https://doi.org/10.1038/nmeth.2109.

Dobin, A., Davis, C.A., Schlesinger, F., Drenkow, J., Zaleski, C., Jha, S., Batut, P., Chaisson, M., Gingeras, T.R., 2013. STAR: ultrafast universal RNA-seq aligner. Bioinformatics 29, 15–21. https://doi.org/10.1093/bioinformatics/bts635.

Drechsler, C., 1933. Morphological features of some more fungi that capture and kill nematodes. J. Wash. Acad. Sci. 23, 267–270.

Finn, R.D., Attwood, T.K., Babbitt, P.C., Bateman, A., Bork, P., Bridge, A.J., Chang, H.-Y., Dosztányi, Z., El-Gebali, S., Fraser, M., Gough, J., Haft, D., Holliday, G.L., Huang, H., Huang, X., Letunic, I., Lopez, R., Lu, S., Marchler-Bauer, A., Mi, H., Mistry, J., Natale, D.A., Necci, M., Nuka, G., Orengo, C.A., Park, Y.M., Pesseat, S., Piovesan, D., Potter, S.C., Rawlings, N.D., Redaschi, N., Richardson, L.J., Rivoire, C., Sangrador-Vegas, A., Sigrist, C.J.A., Sillitoe, I.P.W., Smithers, B., Squizzato, S., Sutton, G.G., Thanki, N., Thomas, P.D., Tosatto, S.C.E., Wu, C.H., Xenarios, I., Yeh, L.-S.-L., Yong, S.-Y., Mitchell, A.L., 2016. InterPro in 2017—beyond protein family and domain annotations. Nucleic Acids Res. 45, D190–D199.

Futai, K., 2013. Pine wood nematode, *Bursaphelenchus xylophilus*. Annu. Rev. Phytopathol. 51, 61–83. https://doi.org/10.1146/annurev-phyto-081211-172910.

Gardes, M., Bruns, T.D., 1993. ITS primers with enhanced specificity for basidiomycetes-application to the identification of mycorrhizae and rusts. Mol. Ecol. 2, 113–118. https://doi.org/10.1111/j.1365-294X.1993.tb00005.x.

Gong, S., Meng, Q., Qiao, J., Zhong, W., Huang, Y., Zhang, G., Chen, Y., Cai, X., 2019. Gene cloning and bioactivity analysis of chitinase gene AO-483 from *Arthrobotrys oligospora* XJ-A1. Acta Agric. Zhejiangensis. 31, 222–228. https://doi.org/10.3969/j.issn.1004-1524.2019.02.07.

Gong, S., Meng, Q., Qiao, J., Huang, Y., Zhong, W., Zhang, G., Zhang, K., Li, N., Shang, Y., Li, Z., Cai, X., 2022. Biological Characteristics of Recombinant *Arthrobotrys oligospora* Chitinase AO-801. Korean J. Parasitol. 60, 345–352. https://doi.org/10.3347/kjp.2022.60.5.345.

Griffiths-Jones, S., Moxon, S., Marshall, M., Khanna, A., Eddy, S.R., Bateman, A., 2005. Rfam: annotating non-coding RNAs in complete genomes. Nucleic Acids Res. 33, D121–D124. https://doi.org/10.1093/nar/gki081.

Haard, K., 1968. Taxonomic studies on the genus *Arthrobotrys* Corda. Mycologia 60, 1140–1159. https://doi.org/10.1080/00275514.1968.12018681.

Haas, B.J., Salzberg, S.L., Zhu, W., Pertea, M., Allen, J.E., Orvis, J., White, O., Buell, C.R., Wortman, J.R., 2008. Automated eukaryotic gene structure annotation using EVidenceModeler and the program to Assemble Spliced Alignments. Genome Biol. 9, R7. https://doi.org/10.1186/gb-2008-9-1-r7.

He, Z.Q., Wang, L.J., Wang, Y.J., Chen, Y.H., Wen, Y., Zhang, K.Q., Niu, X.M., 2021. Polyketide synthase-terpenoid synthase hybrid pathway regulation of trap formation through ammonia metabolism controls soil colonization of predominant nematode-trapping fungus. J. Agric. Food Chem. 69, 4464–4479. https://doi.org/10.1021/acs.jafc.1c00771.

Huerta-Cepas, J., Forslund, K., Coelho, L.P., Szklarczyk, D., Jensen, L.J., von Mering, C., Bork, P., 2017. Fast genome-wide functional annotation through orthology assignment by eggNOG-mapper. Mol. Biol. Evol. 34, 2115–2122. https://doi.org/10.1093/molbev/msx148.

Hussain, T., Ozair, M., Aslam, A., Jameel, S., Nawaz, M., Abdel-Aty, A.-H., 2022. Mathematical study of nematode transmission in pine trees through bark beetles. Chaos, Solitons Fractals 161, 112297. https://doi.org/10.1016/j.chaos.2022.112297.

Jacobs, K., Bergdahl, D.R., Wingfield, M.J., Halik, S., Seifert, K.A., Bright, D.E., Wingfield, B.D., 2004. *Leptographium wingfieldii* introduced into North America and found associated with exotic *Tomicus piniperda* and native bark beetles. Mycol. Res. 108, 411–418. https://doi.org/10.1017/S0953756204009748.

Jia, H., Wang, F., Liu, X., and Li, D., 2023. The AL-ao379 gene plays a role in promoting the invasion stage of *Bursaphelenchus xylophilus* trapped by *Arthrobotrys cladodes*. Preprint. DOi: 10.21203/rs.3.rs-3077296/.

Jia, H., Xia, R., Zhang, R., Liang, G., Zhuang, Y., Zhou, Y., Li, D., Wang, F., 2024. Transcriptome analysis highlights the influence of temperature on hydrolase and traps in nematode-trapping fungi. Front. Microbiol. 15, 1384459. https://doi.org/10.3389/fmicb.2024.1384459.

Kapitonov, V.V., Jurka, J., 2008. A universal classification of eukaryotic transposable elements implemented in Repbase. Nat. Rev. Genet. 9, 411–412. https://doi.org/10.1038/nrg2165-c1.

Kassam, R., Yadav, J., Chawla, G., Kundu, A., Hada, A., Jaiswal, N., Bollinedi, H., Kamil, D., Devi, P., Rao, U., 2021. Identification, characterization, and evaluation of nematophagous fungal species of *Arthrobotrys* and *Tolypocladium* for the management of *Meloidogyne incognita*. Front. Microbiol. 12, 790223. https://doi.org/10.3389/fmicb.2021.790223.

Katoh, K., Standley, D.M., 2013. MAFFT multiple sequence alignment software version 7: improvements in performance and usability. Mol. Biol. Evol. 30, 772–780. https://doi.org/10.1093/molbev/mst010.

Kim, B.-N., Kim, J.H., Ahn, J.-Y., Kim, S., Cho, B.-K., Kim, Y.-H., Min, J., 2020. A short review of the pinewood nematode, Bursaphelenchus Xylophilus. Toxicol. Environ. Health Sci. 12, 297–304. https://doi.org/10.1007/s13530-020-00068-0.

Krogh, A., Brown, M., Mian, I.S., Sjölander, K., Haussler, D., 1994. Hidden Markov models in computational biology: applications to protein modeling. J. Mol. Biol. 235, 1501–1531. https://doi.org/10.1006/jmbi.1994.1104.

Kück, P., Meusemann, K., 2010. FASconCAT: convenient handling of data matrices. Mol. Phylogenet. Evol. 56, 1115–1118. https://doi.org/10.1016/j.ympev.2010.04.024.

Kumar, S., Stecher, G., Li, M., Knyaz, C., Tamura, K., 2018. MEGA X: molecular evolutionary genetics analysis across computing platforms. Mol. Biol. Evol. 35, 1547–1549. https://doi.org/10.1093/molbev/msy096.

Kuthubutheen, A.J., Muid, S., Webster, J., 1985. *Arthrobotrys dendroides*, a new nematode-trapping synnematous *Arthrobotrys* from Malaysia. Trans. Br. Mycol. Soc. 84, 563–566. https://doi.org/10.1016/S0007-1536(85)80028-0.

Lagesen, K., Hallin, P., Rødland, E.A., Stærfeldt, H.-H., Rognes, T., Ussery, D.W., 2007. RNAmmer: consistent and rapid annotation of ribosomal RNA genes. Nucleic Acids Res. 35, 3100–3108. https://doi.org/10.1093/nar/gkm160.

Lehenberger, M., Benkert, M., Biedermann, P.H.W., 2021. Ethanol-enriched substrate facilitates ambrosia beetle fungi, but inhibits their pathogens and fungal symbionts of barkbeetles. Front. Microbiol. 11, 590111. https://doi.org/10.3389/fmicb.2020.590111.

Li, N., Sun, Y., Liu, Y., Wei, L., Zhang, J., Li, N., Sun, D., Jiao, J., Zuo, Y., Li, R., 2024. Expression profiles and characterization of microRNAs responding to chitin in *Arthrobotrys oligospora*. Arch. Microbiol. 206, 1–13. https://doi.org/10.1007/s00203-024-03949-x.

Li, Y., Hyde, K.D., Jeewon, R., Cai, L., Vijaykrishna, D., Zhang, K., 2005. Phylogenetics and evolution of nematode-trapping fungi (Orbiliales) estimated from nuclear and protein coding genes. Mycologia 97, 1034–1046. https://doi.org/10.1080/15572536.2006.11832753.

Liang, L., Wu, H., Liu, Z., Shen, R., Gao, H., Yang, J., Zhang, K., 2013. Proteomic and transcriptional analyses of *Arthrobotrys oligospora* cell wall related proteins reveal complexity of fungal virulence against nematodes. Appl. Microbiol. Biotechnol. 97, 8683–8692. https://doi.org/10.1007/s00253-013-5178-1.

Lin, H.-C., de Ulzurrun, G.-V.-D., Chen, S.-A., Yang, C.-T., Tay, R.J., Iizuka, T., Huang, T.-Y., Kuo, C.-Y., Gonçalves, A.P., Lin, S.-Y., Chang, Y.-C., Stajich, J.E., Schwarz, E.M., Hsueh, Y.-P., 2023. Key processes required for the different stages of fungal carnivory by a nematode-trapping fungus. PLoS Biol. 21, e3002400. https://doi.org/10.1371/journal.pbio.3002400.

Liu, T., Huang, Y., Chen, X.-X., Long, X., Yang, Y.-H., Zhu, M.-L., Mo, M.-H., Zhang, K.-Q., 2020. Comparative transcriptomics reveals features and possible mechanisms of glucose-mediated soil fungistasis relief in *Arthrobotrys oligospora*. Front. Microbiol. 10, 3143. https://doi.org/10.3389/fmicb.2019.03143.

Liu, Y.J., Whelen, S., Hall, B.D., 1999. Phylogenetic relationships among ascomycetes: evidence from an RNA polymerse II subunit. Mol. Biol. Evol. 16, 1799–1808. https://doi.org/10.1093/oxfordjournals.molbev.a026092.

Lowe, T.M., Eddy, S.R., 1997. tRNAscan-SE: a program for improved detection of transfer RNA genes in genomic sequence. Nucleic Acids Res. 25, 955–964. https://doi.org/10.1093/nar/25.5.955.

Lu, T., Yao, B., and Zhang, C., 2012. DFVF: database of fungal virulence factors. Database (Oxford) 2012, bas032. DOi: 10.1093/database/bas032.

Luo, R., Liu, B., Xie, Y., Li, Z., Huang, W., Yuan, J., He, G., Chen, Y., Pan, Q., Liu, Y., Tang, J., Wu, G., Zhang, H., Shi, Y., Liu, Y., Yu, C., Wang, B., Lu, Y., Han, C., Cheung, D.W., Yiu, S.-M., Peng, S., Xiaoqian, Z., Liu, G., Liao, X., Li, Y., Yang, H., Wang, J., Lam, T.-W., Wang, J., 2012. SOAPdenovo2: an empirically improved memory-efficient short-read *de novo* assembler. GigaScience 1, 18. https://doi.org/10.1186/2047-217X-1-18.

Majoros, W.H., Pertea, M., Salzberg, S.L., 2004. TigrScan and GlimmerHMM: two open source ab initio eukaryotic gene-finders. Bioinformatics 20, 2878–2879. https://doi.org/10.1093/bioinformatics/bth315.

Marincowitz, S., Duong, T.A., De Beer, Z.W., Wingfield, M.J., 2015. *Cornuvesica*: a little known mycophilic genus with a unique biology and unexpected new species. Fungal Biol. 119, 615–630. https://doi.org/10.1016/j.funbio.2015.03.007.

McArthur, A.G., Waglechner, N., Nizam, F., Yan, A., Azad, M.A., Baylay, A.J., Bhullar, K., Canova, M.J., De Pascale, G., Ejim, L., Kalan, L., King, A.M., Koteva, K., Morar, M., Mulvey, M.R., O'Brien, J.S., Pawlowski, A.C., Piddock, L.J., Spanogiannopoulos, P., Sutherland, A.D., Tang, I., Taylor, P.L., Thaker, M., Wang, W., Yan, M., Yu, T., Wright, G.D., 2013. The comprehensive antibiotic resistance database. Antimicrob. Agents Chemother. 57, 3348–3357. https://doi.org/10.1128/aac.00419-13.

Miller, G.L., 1959. Use of dinitrosalicylic acid reagent for determination of rreducing sugar. Anal. Chem. 31, 426–428. https://doi.org/10.1021/ac60147a030.

Miller, M.A., Pfeiffer, W., Schwartz, T., 2010. Creating the CIPRES Science Gateway for inference of large phylogenetic trees. In: Gateway Computing Environments Workshop (GCE). Institute of Electrical and Electronics Engineers, New Orleans, LA, pp. 1–8.

Moriya, Y., Itoh, M., Okuda, S., Yoshizawa, A.C., Kanehisa, M., 2007. KAAS: an automatic genome annotation and pathway reconstruction server. Nucleic Acids Res. 35, W182–W185. https://doi.org/10.1093/nar/gkm321.

Naz, I., Khan, R.A.A., Masood, T., Baig, A., Siddique, I., Haq, S., 2021. Biological control of root knot nematode, *Meloidogyne incognita*, in vitro, greenhouse and field in

cucumber. Biol. Control 152, 104429. https://doi.org/10.1016/j.biocontrol.2020.104429.
Nourani, S.L., Goltapeh, E., Safaie, N., Jalali Javaran, M., Pourjam, E., Shams-bakhsh, M., Afshar, F., 2015. The effects of *Arthrobotrys oligospora* and *Arthrobotrys conoides* culture filtrates on second stage juvenile mortality and egg hatching of *Meloidogyne incognita* and *Meloidogyne javanica*.J. Crop Prot. 2015, 667–674.
Noweer, E., 2014. Evaluation of nematophagous fungi dactylaria brochopaga and *Arthrobotrys dactyloides* against *Meloidogyne incognita* infesting peanut plants under field conditions. Agric. Biol. J. N. Am. 5, 193–197. https://doi.org/10.5251/abjna.2014.5.5.193.197.
Özdemir, G.G.F., Arici, E., 2021. Effect of culture filtrate concentration of *Rhizoctonia solani* Kühn against *Meloidogyne incognita* and *Meloidogyne hapla* in vitro. Int. J. Agric. for. Life Sci. 5, 74–79.
Pérez-Anzúrez, G., Olmedo-Juárez, A., von-Son de Fernex, E., Alonso-Díaz, M. Á., Delgado-Núñez, E. J., López-Arellano, M. E., González-Cortázar, M., Zamilpa, A., Ocampo-Gutierrez, A. Y., Paz-Silva, A., and Mendoza-de Gives, P., 2022. *Arthrobotrys musiformis* (Orbiliales) kills *Haemonchus contortus* infective larvae (Trichostronylidae) through its predatory activity and its fungal culture filtrates. Pathogens. 11, 1068. DOi: 10.3390/pathogens11101068.
Price, A.L., Jones, N.C., Pevzner, P.A., 2005. De novo identification of repeat families in large genomes. Bioinformatics 21 (Suppl. 1), i351–i358. https://doi.org/10.1093/bioinformatics/bti1018.
Rahman, M.U., Chen, P., Zhang, X., Fan, B., 2023. Predacious strategies of nematophagous fungi as bio-control agents. Agronomy 13, 2685. https://doi.org/10.3390/agronomy13112685.
Ramesh, P., Reena, P., Amitbikram, M., Chaitanya, J., Anju, K., 2015. Insight into the transcriptome of *Arthrobotrys conoides* using high throughput sequencing. J. Basic Microbiol. 55, 1394–1405. https://doi.org/10.1002/jobm.201500237.
Resnerová, K., Schovánková, J., Horák, J., Holuša, J., 2022. Relationships between the fecundity of bark beetles and the presence of antagonists. Sci. Rep. 12, 7573. https://doi.org/10.1038/s41598-022-11630-w.
Ronquist, F., Teslenko, M., van der Mark, P., Ayres, D.L., Darling, A., Höhna, S., Larget, B., Liu, L., Suchard, M.A., Huelsenbeck, J.P., 2012. MrBayes 3.2: efficient Bayesian phylogenetic inference and model choice across a large model space. Syst. Biol. 61, 539–542. https://doi.org/10.1093/sysbio/sys029.
Ryss, A.Y., Subbotin, S.A., 2023. New records of wood- and bark-inhabiting nematodes from woody plants with a description of *Bursaphelenchus zvyagintsevi* sp. n. (aphelenchoididae: Parasitaphelenchinae) from Russia. Plants 12, 382. https://doi.org/10.3390/plants12020382.
Schenck, S., Kendrick, W.B., Pramer, D., 1977. A new nematode-trapping hyphomycete and a reevaluation of *Dactylaria* and *Arthrobotrys*. Can. J. Bot. 55, 977–985. https://doi.org/10.1139/b77-115.
Schenck, S., Chase, T., Rosenzweig, W.D., Pramer, D., 1980. Collagenase production by nematode-trapping fungi. Appl. Environ. Microbiol. 40, 567–570. https://doi.org/10.1128/aem.40.3.567-570.1980.
Schubert, M., Lindgreen, S., Orlando, L., 2016. AdapterRemoval v2: rapid adapter trimming, identification, and read merging. BMC. Res. Notes 9, 88. https://doi.org/10.1186/s13104-016-1900-2.
Slater, G.S.C., Birney, E., 2005. Automated generation of heuristics for biological sequence comparison. BMC Bioinf. 6, 31. https://doi.org/10.1186/1471-2105-6-31.
Smit, A. F. A., and Hubley, R. RepeatModeler Open-1.0 (2008–2015).
Song, T.-Y., Xu, Z.-F., Chen, Y.-H., Ding, Q.-Y., Sun, Y.-R., Miao, Y., Zhang, K.-Q., Niu, X.-M., 2017. Potent nematicidal activity and new hybrid metabolite production by disruption of a cytochrome P450 gene involved in the biosynthesis of morphological regulatory arthrosporols in nematode-trapping fungus *Arthrobotrys oligospora*. J. Agric. Food Chem. 65, 4111–4120. https://doi.org/10.1021/acs.jafc.7b01290.
Stamatakis, A., 2014. RAxML version 8: a tool for phylogenetic analysis and post-analysis of large phylogenies. Bioinformatics 30, 1312–1313. https://doi.org/10.1093/bioinformatics/btu033.
Stanke, M., Morgenstern, B., 2005. AUGUSTUS: a web server for gene prediction in eukaryotes that allows user-defined constraints. Nucleic Acids Res. 33, W465–W467. https://doi.org/10.1093/nar/gki458.
Tamura, K., Stecher, G., Peterson, D., Filipski, A., Kumar, S., 2013. MEGA6: molecular evolutionary genetics analysis version 6.0. Mol. Biol. Evol. 30, 2725–2729. https://doi.org/10.1093/molbev/mst197.
Tempel, S., 2012. Using and understanding RepeatMasker. Pages 29–51 in: Mobile Genetic Elements: Protocols and Genomic Applications. Y. Bigot, ed. Humana Press, Totowa, NJ.
Teng, L.-L., Song, T.-Y., Chen, Y.-H., Chen, Y.-G., Zhang, K.-Q., Li, S.-H., Niu, X.-M., 2020. Novel polyketide-terpenoid hybrid metabolites from a potent nematicidal *Arthrobotrys oligospora* mutant ΔAOL_s00215g278. J. Agric. Food Chem. 68, 11449–11458. https://doi.org/10.1021/acs.jafc.0c04713.
Ter-Hovhannisyan, V., Lomsadze, A., Chernoff, Y.O., Borodovsky, M., 2008. Gene prediction in novel fungal genomes using an ab initio algorithm with unsupervised training. Genome Res. 18, 1979–1990. https://doi.org/10.1101/gr.081612.108.
Tranier, M.-S., Pognant-Gros, J., Quiroz, R.D.I.C., González, C.N.A., Mateille, T., Roussos, S., 2014. Commercial biological control agents targeted against plant-parasitic root-knot nematodes. Braz. Arch. Biol. Technol. 57, 831–841. https://doi.org/10.1590/S1516-8913201402540.
Tunlid, A., Rosén, S., Ek, B., Rask, L., 1994. Purification and characterization of an extracellular serine protease from the nematode-trapping fungus *Arthrobotrys oligospora*. Microbiology 140, 1687–1695. https://doi.org/10.1099/13500872-140-7-1687.
Vidal-Diez de Ulzurrun, G., Juan, S.-C., Lin, T.-H., and Hsueh, Y.-P., 2024. Nematode-trapping fungi and *Caenorhabditis elegans* as a model system for predator–prey interactions. Pages 273–292 in: Fungal Associations. Y.-P. Hsueh and M. Blackwell, eds. Springer International Publishing, Cham.
Walker, B.J., Abeel, T., Shea, T., Priest, M., Abouelliel, A., Sakthikumar, S., Cuomo, C.A., Zeng, Q., Wortman, J., Young, S.K., Earl, A.M., 2014. Pilon: an integrated tool for comprehensive microbial variant detection and genome assembly improvement. PLoS One 9, e112963. https://doi.org/10.1371/journal.pone.0112963.
Wang, D., Ma, N., Rao, W., Zhang, Y., 2023. Recent advances in life history transition with nematode-trapping fungus *Arthrobotrys oligospora* and its application in sustainable agriculture. Pathogens 12, 367. https://doi.org/10.3390/pathogens12030367.
Wang, F., Pang, Y., 1981. Condition experiments for the determination of protease activity using the Folin-phenol reagent method. Flavor Condiment Sci. Technol. 12, 21–24.
Wang, L., Feng, Z., Wang, X., Wang, X., Zhang, X., 2010. DEGseq: an R package for identifying differentially expressed genes from RNA-seq data. Bioinformatics 26, 136–138. https://doi.org/10.1093/bioinformatics/btp612.
Wang, M., Yang, J., Zhang, K.-Q., 2006a. Characterization of an extracellular protease and its cDNA from the nematode-trapping fungus *Monacrosporium microscaphoides*. Can. J. Microbiol. 52, 130–139. https://doi.org/10.1139/w05-110.
Wang, R.B., Yang, J.K., Lin, C., Zhang, Y., Zhang, K.Q., 2006b. Purification and characterization of an extracellular serine protease from the nematode-trapping fungus *Dactylella shizishanna*. Lett. Appl. Microbiol. 42, 589–594. https://doi.org/10.1111/j.1472-765X.2006.01908.x.
Waterhouse, R.M., Seppey, M., Simão, F.A., Manni, M., Ioannidis, P., Klioutchnikov, G., Kriventseva, E.V., Zdobnov, E.M., 2018. BUSCO applications from quality assessments to gene prediction and phylogenomics. Mol. Biol. Evol. 35, 543–548. https://doi.org/10.1093/molbev/msx319.
White, T. J., Bruns, T., Lee, S., and Taylor, J. W., 1990. Amplification and direct sequencing of fungal ribosomal RNA genes for phylogenetics. Pages 315-322 in: PCR protocols: a guide to methods and applications. M. A. Innis, D. H. Gelfand, J. J. Sninsky and T. J. White, eds. Academic Press, San Diego (California).
Wu, Y., Yang, Z., Jiang, Z., Nizamani, M.M., Zhang, H., Liu, M., Wei, S., Wang, Y., Li, K., 2023. Isolation, identification, and evaluation of the predatory activity of Chinese *Arthrobotrys* species towards economically important plant-parasitic nematodes. J. Fungi. 9, 1125. https://doi.org/10.3390/jof9121125.
Xiao, Y., Guo, Q., Xie, N., Yuan, G., Liao, M., Gui, Q., Ding, G., 2024. Predicting the global potential distribution of *Bursaphelenchus xylophilus* using an ecological niche model: expansion trend and the main driving factors. BMC Ecol. Evol. 24, 48. https://doi.org/10.1186/s12862-024-02234-1.
Xu, Z.-F., Chen, Y.-H., Song, T.-Y., Zeng, Z.-J., Yan, N., Zhang, K.-Q., Niu, X.-M., 2016. Nematicidal key precursors for the biosynthesis of morphological regulatory arthrosporols in the nematode-trapping fungus *Arthrobotrys oligospora*. J. Agric. Food Chem. 64, 7949–7956. https://doi.org/10.1021/acs.jafc.6b03241.
Yang, E., Xu, L., Yang, Y., Zhang, X., Xiang, M., Wang, C., An, Z., Liu, X., 2012. Origin and evolution of carnivorism in the Ascomycota (fungi). Proc. Natl. Acad. Sci. 109, 10960–10965. https://doi.org/10.1073/pnas.1120915109.
Yang, J., Tian, B., Liang, L., Zhang, K.Q., 2007a. Extracellular enzymes and the pathogenesis of nematophagous fungi. Appl. Microbiol. Biotechnol. 75, 21–31. https://doi.org/10.1007/s00253-007-0881-4.
Yang, J., Li, J., Liang, L., Tian, B., Zhang, Y., Cheng, C., Zhang, K.Q., 2007b. Cloning and characterization of an extracellular serine protease from the nematode-trapping fungus *Arthrobotrys conoides*. Arch. Microbiol. 188, 167–174. https://doi.org/10.1007/s00203-007-0233-x.
Yang, J., Wang, L., Ji, X., Feng, Y., Li, X., Zou, C., Xu, J., Ren, Y., Mi, Q., Wu, J., Liu, S., Liu, Y., Huang, X., Wang, H., Niu, X., Li, J., Liang, L., Luo, Y., Ji, K., Zhou, W., Yu, Z., Li, G., Liu, Y., Li, L., Qiao, M., Feng, L., Zhang, K.Q., 2011. Genomic and proteomic analyses of the fungus *Arthrobotrys oligospora* provide insights into nematode-trap formation. PLoS Pathog. 7, e1002179. https://doi.org/10.1371/journal.ppat.1002179.
Yang, L., Li, X., Bai, N., Yang, X., Zhang, K.Q., Yang, J., 2022. Transcriptomic analysis reveals that Rho GTPases regulate trap development and lifestyle transition of the nematode-trapping fungus *Arthrobotrys oligospora*. Microbiol. Spectr. 10. https://doi.org/10.1128/spectrum.01759-21 e01759-01721.
Yu, G., Wang, L.G., Han, Y., He, Q.Y., 2012. clusterProfiler: an R package for comparing biological themes among gene clusters. OMICS 16, 284–287. https://doi.org/10.1089/omi.2011.0118.
Zhang, F., Boonmee, S., Bhat, J.D., Xiao, W., Yang, X.Y., 2022a. New *Arthrobotrys* nematode-trapping species (Orbiliaceae) from terrestrial soils and freshwater sediments in China. J. Fungi. 8, 671. https://doi.org/10.3390/jof807067.
Zhang, F., Boonmee, S., Yang, Y.-Q., Zhou, F.-P., Xiao, W., Yang, X., 2023a. *Arthrobotrys blastospora* sp. nov. (Orbiliomycetes): a living fossil displaying morphological traits of mesozoic carnivorous fungi. J. Fungi. 9, 451. https://doi.org/10.3390/jof9040451.
Zhang, F., Yang, Y.-Q., Zhou, F.-P., Xiao, W., Boonmee, S., Yang, X.Y., 2023b. Morphological and phylogenetic characterization of five novel nematode-trapping fungi (Orbiliomycetes) from Yunnan. China. J. Fungi. 9, 735. https://doi.org/10.3390/jof9070735.
Zhang, F., Yang, Y.-Q., Zhou, F.-P., Xiao, W., Boonmee, S., Yang, X.Y., 2024a. Multilocus phylogeny and characterization of five undescribed aquatic carnivorous fungi (Orbiliomycetes). J. Fungi. 10, 81. https://doi.org/10.3390/jof10010081.
Zhang, H., Wei, Z., Zhang, J., Liu, X., 2021. Classification of dendrocola nematode-trapping fungi. J. For. Res. 32, 1295–1304. https://doi.org/10.1007/s11676-020-01159-x.
Zhang, H., Wei, Z., Liu, X., Zhang, J., Diao, G., 2022b. Growth and decline of arboreal fungi that prey on *Bursaphelenchus xylophilus* and their predation rate. J. For. Res. 33, 699–709. https://doi.org/10.1007/s11676-021-01334-8.

Zhang, J.-H., Zhang, H.-M., Ma, X.-X., Sun, Y.-S., Li, R.-B., Li, N.-X., Cai, X.-P., Qiao, J., Meng, Q.-L., 2024b. Degradation on nematodes of chitinase AO-492 from *Arthrospora oligospora*. Biotechnol. Bull. 40, 152–160.

Zhang, J.-Y., Hyde, K.D., Zhang, L.-J., Bai, S., Bao, D.-F., Al-Otibi, F., Lu, Y.-Z., 2025a. Two novel hyphomycetes associated with ferns from China. MycoKeys 113, 101–121. https://doi.org/10.3897/mycokeys.113.137678.

Zhang, J., Wei, L., Zhang, H., Ma, X., Sun, Y., Li, R., Zhang, C., Cai, X., Qiao, J., Meng, Q., 2025b. Proteomic insights into nematode-trapping fungi *Arthrobotrys oligospora* after their response to chitin. J. Vet. Res. 69, 71–82. https://doi.org/10.2478/jvetres-2025-0005.

Zhang, K.-Q., Hyde, K.D., 2014. Nematode-trapping fungi. Springer Science & Business.

Zhang, W., Fan, Y., Deng, W., Chen, Y., Wang, S., Kang, S., Steenwyk Jacob, L., Xiang, M., and Liu, X., 2024c. Characterization of genome-wide phylogenetic conflict uncovers evolutionary modes of carnivorous fungi. mBio. 15, e02133-02124. DOi: 10.1128/mbio.02133-24.

Zhao, M., Mo, M., Zhang, K., 2004. Characterization of a neutral serine protease and its full-length cDNA from the nematode-trapping fungus *Arthrobotrys oligospora*. Mycologia 96, 16–22. https://doi.org/10.1080/15572536.2005.11832991.

Zhong, W., Ying, C., Shasha, G., Jun, Q., Qingling, M., Zhang, X., Xifeng, W., Huang, Y., Lulu, T., Yanbing, N., 2019. Enzymological properties and nematode-degrading activity of recombinant chitinase AO-379 of *Arthrobotrys oligospora*. Kafkas Üniversitesi Veteriner Fakültesi Dergisi. 25, 534. https://doi.org/10.9775/kvfd.2018.20603.

Zhou, J., Wu, Q.-F., Li, S.-H., Yan, J.-X., Wu, L., Cheng, Q.-Y., He, Z.-Q., Yue, X.-T., Zhang, K.-Q., Zhang, L.-L., Niu, X.-M., 2022. The multifaceted gene 275 embedded in the PKS-PTS gene cluster was involved in the regulation of arthrobotrisin biosynthesis, TCA Cycle, and septa formation in nematode-trapping fungus *Arthrobotrys oligospora*. J. Fungi. 8, 1261. https://doi.org/10.3390/jof8121261.